Research paper

A comprehensive antigen production and characterisation study for easy-to-implement, specific and quantitative SARS-CoV-2 serotests

Miriam Klausberger[a,1], Mark Duerkop[a,b,1], Helmuth Haslacher[c], Gordana Wozniak-Knopp[a,d], Monika Cserjan-Puschmann[a,e], Thomas Perkmann[c], Nico Lingg[a,e], Patricia Pereira Aguilar[a,e], Elisabeth Laurent[a,f], Jelle De Vos[a,g], Manuela Hofner[h], Barbara Holzer[i], Maria Stadler[j], Gabriele Manhart[k], Klemens Vierlinger[h], Margot Egger[l], Lisa Milchram[h], Elisabeth Gludovacz[a], Nicolas Marx[a], Christoph Köppl[a,e], Christopher Tauer[a], Jürgen Beck[a], Daniel Maresch[m], Clemens Grünwald-Gruber[m,n], Florian Strobl[o], Peter Satzer[a,e], Gerhard Stadlmayr[a,d], Ulrike Vavra[p], Jasmin Huber[h], Markus Wahrmann[q], Farsad Eskandary[q], Marie-Kathrin Breyer[r], Daniela Sieghart[s], Peter Quehenberger[c], Gerda Leitner[t], Robert Strassl[c], Alexander E. Egger[u], Christian Irsara[u], Andrea Griesmacher[u], Gregor Hoermann[u,v], Günter Weiss[w], Rosa Bellmann-Weiler[w], Judith Loeffler-Ragg[w,2], Nicole Borth[a], Richard Strasser[p], Alois Jungbauer[a,e], Rainer Hahn[a,e], Jürgen Mairhofer[o], Boris Hartmann[i], Nikolaus B. Binder[x], Gerald Striedner[a,b,e,o], Lukas Mach[p], Andreas Weinhäusel[h], Benjamin Dieplinger[l], Florian Grebien[k,*], Wilhelm Gerner[j,y,z,1], Christoph J. Binder[c,1,*], Reingard Grabherr[a,1,*]

[a] Department of Biotechnology, University of Natural Resources and Life Sciences (BOKU) Vienna, Muthgasse 18, 1190 Vienna, Austria
[b] Novasign GmbH Vienna, Austria
[c] Department of Laboratory Medicine, Medical University of Vienna, Währinger Gürtel 18-20, 1090 Vienna, Austria
[d] CD Laboratory for innovative Immunotherapeutics, Vienna, Austria
[e] ACIB-Austrian Centre of Industrial Biotechnology, Graz, Austria
[f] BOKU Core Facility Biomolecular & Cellular Analysis, University of Natural Resources and Life Sciences (BOKU),Vienna, Austria
[g] Department of Chemical Engineering, Vrije Universiteit Brussel (VUB), Brussels, Belgium
[h] Competence Unit Molecular Diagnostics, Center for Health and Bioresources, AIT Austrian Institute of Technology GmbH, Vienna, Austria
[i] Austrian Agency for Health and Food Safety (AGES), Department for Animal Health, Moedling, Austria
[j] Institute of Immunology, University of Veterinary Medicine, Vienna, Austria
[k] Institute for Medical Biochemistry, University of Veterinary Medicine, Veterinärplatz 1, 1210 Vienna, Austria
[l] Department of Laboratory Medicine, Konventhospital Barmherzige Brueder Linz and Ordensklinikum Linz Barmherzige Schwestern, Linz, Austria
[m] BOKU Core Facility Mass Spectrometry, University of Natural Resources and Life Sciences (BOKU), Vienna, Austria
[n] Department of Chemistry, University of Natural Resources and Life Sciences (BOKU) Vienna, Austria
[o] enGenes Biotech GmbH, Vienna, Austria
[p] Department of Applied Genetics and Cell Biology, University of Natural Resources and Life Sciences (BOKU) Vienna, Austria
[q] Department of Medicine III, Division of Nephrology and Dialysis, Medical University of Vienna, Austria
[r] Department of Respiratory and Critical Care Medicine and Ludwig Boltzmann Institute for Lung Health, Otto Wagner Hospital, Vienna, Austria
[s] Division of Rheumatology, Department of Medicine III, Medical University of Vienna, Austria
[t] Department of Blood Group Serology and Transfusion Medicine, Medical University of Vienna, Austria
[u] Central Institute for Medical and Chemical Laboratory Diagnosis, Innsbruck University Hospital, Innsbruck, Austria
[v] MLL Munich Leukemia Laboratory, Munich, Germany
[w] Department of Internal Medicine II, Innsbruck Medical University, Innsbruck, Austria
[x] Technoclone Herstellung von Diagnostika und Arzneimitteln GmbH, Vienna, Austria
[y] Christian Doppler Laboratory for an Optimized Prediction of Vaccination Success in Pigs, University of Veterinary Medicine, Vienna, Austria
[z] Present address: The Pirbright Institute, Pirbright, United Kingdom

A B S T R A C T

Background: Antibody tests are essential tools to investigate humoral immunity following SARS-CoV-2 infection or vaccination. While first-generation antibody tests have primarily provided qualitative results, accurate seroprevalence studies and tracking of antibody levels over time require highly specific, sensitive and quantitative test setups.

Methods: We have developed two quantitative, easy-to-implement SARS-CoV-2 antibody tests, based on the spike receptor binding domain and the nucleocapsid protein. Comprehensive evaluation of antigens from several biotechnological platforms enabled the identification of superior antigen designs for reliable serodiagnostic. Cut-off modelling based on unprecedented large and heterogeneous multicentric validation cohorts allowed us to define optimal thresholds for the tests' broad applications in different aspects of clinical use, such as seroprevalence studies and convalescent plasma donor qualification.

Findings: Both developed serotests individually performed similarly-well as fully-automated CE-marked test systems. Our described sensitivity-improved orthogonal test approach assures highest specificity (99.8%); thereby enabling robust serodiagnosis in low-prevalence settings with simple test formats. The inclusion of a calibrator permits accurate quantitative monitoring of antibody concentrations in samples collected at different time points during the acute and convalescent phase of COVID-19 and disclosed antibody level thresholds that correlate well with robust neutralization of authentic SARS-CoV-2 virus.

Interpretation: We demonstrate that antigen source and purity strongly impact serotest performance. Comprehensive biotechnology-assisted selection of antigens and in-depth characterisation of the assays allowed us to overcome limitations of simple ELISA-based antibody test formats based on chromometric reporters, to yield comparable assay performance as fully-automated platforms.

Funding: WWTF, Project No. COV20−016; BOKU, LBI/LBG

Research in context

Evidence before this study

Highly specific, yet sensitive SARS-CoV-2 serodiagnosis for seroprevalence studies or quantitative serotesting almost exclusively relies on fully-automated test platforms, merely available only in well-equipped diagnostic laboratories. Yet, academic research groups and laboratories with basic equipment require access to high-quality test formats for robust and meaningful SARS-CoV-2 seroanalysis. Of note, quantitative high-quality test formats that are easy-to-implement are gaining additional importance as means to characterise the extent of vaccine-induced immunity and to monitor decline of antibody titres over time.

Added value of this study

The present study describes two extensively validated quantitative and highly specific IgG antibody tests that rely on optimised designs of the SARS-CoV-2 receptor binding domain and nucleocapsid protein. In validation studies with unprecedented large and heterogenous multi-centric specificity and sensitivity cohorts, including samples with an increased propensity for cross-reactivity and convalescent sera from SARS-CoV-2-infected individuals covering the full spectrum of clinical manifestations, the simple ELISA-based antibody tests performed equally well or even better than fully automated CE-marked test platforms. Our study highlights that antibody test performance is already influenced as early as by the choice of the antigen production system and discloses process-related peculiarities and parameters that are often underestimated in terms of an antigen for diagnostic use. Moreover, we disclose that false positive and false negative results are highly antigen-dependent. With strategic cut-off modelling and sensitivity-improved orthogonal testing, we provide optimised approaches for different aspects of clinical utility, ranging from serodiagnosis in low-prevalence settings to monitoring antibody levels after infection.

Implications of all the available evidence

Our findings propose that antigen selection and quality are crucial aspects for assay development and may profoundly influence diagnostic performance. A comprehensive approach supported by biotechnological quality attributes aid in improving selectivity of the tests and thereby test performance. Well-characterised, quantitative and simple test formats are urgently needed to support the thorough characterisation of infection- and vaccine-induced antibody responses and their longevity in any research laboratory with minimal equipment. The comprehensively characterised test systems and highly pure antigen reagents described in this study are available from the authors under disclosed addresses.

1. Introduction

Serological testing of severe acute respiratory syndrome coronavirus 2 (SARS-CoV-2) infections remains an essential tool for seroprevalence studies and complements PCR-based diagnosis in identifying asymptomatic individuals [1]. Antibody tests are gaining additional importance as means to characterise the extent of infection- or vaccine-induced immunity. To cope with the urgent demand for sensitive and reliable test systems, many manual and automated serological tests for coronavirus disease 2019 (COVID-19) became available within a short period of time [2]. Owing to the acuity of a spreading pandemic, many of these early developed test systems lacked adequate validation and thereby fuelled mistrust, while stocks of others were exhausted rapidly due to increased demand [3].

Antigen selection and quality are crucial aspects of assay development and influence diagnostic performance [4], such as sensitivity and specificity as well as assay availability, scalability and their field of application. Ideal candidate antigens for *in-vitro* serodiagnosis are highly immunogenic, support early and robust detection of seroconversion after an infection and result in low false positivity rates. Additionally, production platforms supporting high process yields ensure

sustainable assay supply. To date, biotechnological performance attributes and their influence on serodiagnostics have not been reported during the development of assays for SARS-CoV-2 detection. Likewise, no comprehensive study comparing and validating the same SARS-CoV-2 antigen produced in different expression systems with larger cohorts is available.

In this study, we developed two quantitative, enzyme-linked immunosorbent assay (ELISA)-based serotests relying on the SARS-CoV-2 receptor-binding domain (RBD) and nucleocapsid protein (NP) antigens of superior design and quality. Thus far, quantitative tests usually rely on automated test systems. Yet, also minimally-equipped academic and diagnostic laboratories require affordable and high-quality test formats for robust and meaningful SARS-CoV-2 seroanalysis. Since the developed assays utilise established ELISA technology, they are easy to implement in any minimally-equipped lab worldwide. For a simple chromogenic test format with a narrow dynamic measurement range the quality of the diagnostic antigen is particularly important. We describe a comprehensive approach for the first time assessing biotechnological parameters such as antigen quality attributes and manufacturability for an ideal test setup. For this purpose, we compared several animal cell lines and plant-based expression platforms for their ability to support high-quantity and quality RBD production and assessed whether the employed production host influences antigen performance. We extensively validated the tests for clinical utility featuring sera from individuals covering the full spectrum of disease presentations at different time points post infection and a large specificity cohort including samples with antibodies towards endemic human coronaviruses (hCoVs) and those from individuals with underlying non-infectious diseases. Moreover, we validated the tests with time-resolved acute and early convalescent samples from hospitalised patients and showed that only RBD-specific antibodies demonstrate excellent correlation with neutralization assays already in the early phase of infection. Our extensive validation allowed us to define tailor-made test cut-off criteria for the highly diverse fields of clinical applications, which greatly differ in their demands.

2. Methods

2.1. Production of recombinant SARS-CoV-2 antigens for serodiagnosis

2.1.1. Genetic constructs

pCAGGS mammalian expression vectors encoding the canonical SARS-CoV-2 receptor-binding domain (RBD, pCAGGS-RBD, aa Arg319 − Phe541, residue numbering as in NCBI Reference sequence: YP_009724390.1) sequence from the first human isolate Wuhan-1 [5] with a C-terminal hexa-histidine tag, were a kind gift from Florian Krammer, Icahn School of Medicine at Mount Sinai, NY [4]. Both sequences were codon-optimised for the expression in mammalian cells.

A pTT28 mammalian expression vector (National Research Council, NRC, Ottawa, Canada) encoding a truncated version of the SARS-CoV-2 Spike receptor-binding domain (tRBD, pTT28-tRBD, aa Arg319 - Lys537) with a C-terminal octa-histidine tag was generated.

A pEAQ-HT plant expression vector [6] encoding RBD (pEAQ-HT-RBD, aa Arg319 − Phe541) fused to the barley α-amylase signal peptide and a C-terminal hexa-histidine tag was generated. The RBD sequence was codon-optimised for the expression in plants and synthesized by GeneArt (Thermo Fisher Scientific, Regensburg, DE).

A pET30a*cer* E. coli expression vector [7] encoding the full-length SARS-CoV-2 Wuhan-1 NP sequence (aa Met1−Ala419, GenBank: NC_045512.2) [5] fused to a completely removable N-terminal CASPON tag [8,9], yielding pET30a*cer*-CASPON−NP, was generated as described elsewhere [10]. Briefly, SARS-CoV-2 NP sequence was amplified via PCR using the qPCR positive control plasmid 2019-nCoV_N obtained from Integrated DNA Technologies (Coralville,

Iowa, USA) and was fused to the CASPON tag consisting of the negative charged T7AC solubility tag [8], a hexa-histidine tag, a short linker (GSG) and the caspase-2 cleavage site (VDVAD) resulting in the sequence MLEDPERNKERKEAELQAQTAEQHHHHHHGSGVDVAD.

Expression vectors pFUSEss-CHIg-hG1 and pFUSEss2-CLIg-hK, encoding the heavy and light chains of the SARS-CoV/SARS-CoV-2 monoclonal antibody CR3022 [11] were kindly provided by Florian Krammer (Icahn School of Medicine at Mount Sinai, New York, NY).

2.1.2. Large-scale production of transfection-grade plasmid DNA

Plasmid DNA for transient transfection of HEK293−6E cells was produced according to an upstream process described previously [12]. Briefly, the plasmids pCAGGS-RBD and pTT28-tRBD were transformed into E. coli JM108 by electroporation and cultivated in 1-L fed-batch mode. Cells were harvested by centrifugation and pDNA was extracted by alkaline lysis at 5 g/L cellular dry mass (CDM) following a protocol of Urthaler and colleagues [13]. pDNA was processed to >95% purity by multiple chromatography steps based on a platform purification protocol (Cytiva, Little Chalfont, UK) [14].

2.1.3. Transient expression of RBD, tRBD and NP in diverse biotechnological platforms

Human embryonic kidney cells: Shake flask cultivation. HEK293−6E cells (licensed from National Research Council, NRC, Ottawa, Canada) were routinely cultivated in suspension in Freestyle^{TM} F17 medium supplemented with 4 mM L-glutamine, 0.1% (v/v) Pluronic F-68 and 25 μg/mL G-418 (all Thermo Fisher Scientific, Waltham, MA) in a humidified atmosphere of 5−8% (v/v) CO_2 at 37 °C shaking at 125 rpm. Polyethylenimine (PEI)-mediated transient transfections with either pCAGGS-RBD, pTT28-tRBD or pFUSEss-CHIg-hG1 and pFUSEss2-CLIg-hK for the expression or RBD, tRBD or mAb CR3022 were performed according to the manufacturer's protocol as previously described [15,16].

Transfections were performed by dropwise addition of a mixture of one μg plasmid DNA and two μg linear 25-kDa or 40-kDa PEI (Polysciences, Inc., Hirschberg, DE) per mL of culture volume (1.7−2.0 × 10^6 cells/mL). Two- and four-days post-transfection, cells were supplemented with 0.5% (w/V) tryptone N1 (Organotechnie, La Courneuve, FR) and 0.25% (w/V) D (+)-glucose (Carl Roth, Karlsruhe, DE). Supernatants were harvested five to six days post-transfection by centrifugation (2000 g, 15 min) and were filtered through 0.45 μm filters before downstream procedures.

Medium-scale cultivation. Stepwise upscaling was performed using a Multi-bioreactor system DASGIP (Eppendorf, Hamburg, DE) followed by a 10-L scale bioreactor System BioFlo320 (Eppendorf, Hamburg, DE). The bioreactors were inoculated at half the final volume (F17 expression medium supplemented with 4 mM L-Glutamine and 0.1% (v/v) Pluronic) with a seeding density of 0.5 × 10^6 cells/mL. The inoculum was prepared in shake flask cultures as described above. The bioreactors were controlled to a pH of 7.2 using CO_2 and 7.5% (w/V) carbonate base and to 50% (v/v) dissolved oxygen by submerged aeration. Transfection was performed at a cell concentration of 1.7 × 10^6 cells/mL. PEI and the respective plasmid DNA were diluted in media, mixed and incubated at room temperature for ten minutes prior to addition to the cultures (45 μg PEI and 15 μg of plasmid per 10^6 cells). Twenty-four hours post transfection, cells were expanded and 24 h later were fed TN1 peptone at a concentration of 0.5% (v/v). Each day post-transfection viability, cell density and glucose concentration were measured and a daily bolus feed to a glucose concentration of 2.5 g/L was performed. The cultures were harvested once viability dropped below 60%.

Chinese hamster ovary cells: CHO-K1 and CHO-S cells were routinely propagated in CD-CHO medium (Thermo Fisher Scientific, Waltham, MA) or in Hyclone Actipro medium (Cytiva, Chicago, IL) both supplemented with 0.2% (v/v) Anti-Clumping Agent (Thermo Fisher Scientific, Waltham, MA) and 8 mM L-glutamine (CHO-K1, Sigma

Aldrich, St. Louis, MO) or 8 mM GlutaMAX (CHO-S, Thermo Fisher Scientific, Waltham, MA), respectively. Cells were cultivated in suspension at 37 °C, 7% (v/v) CO_2 and humidified air, shaking at 140 rpm.

For nucleofection, a total of 1×10^7 cells in the exponential growth phase were pelleted for eight minutes at 170 g and were resuspended in 99 μL resuspension buffer R (Thermo Fisher Scientific, Waltham, MA). Cells were mixed with pCAGGS-RBD, which had been pre-diluted with UltraPure™ DNase/RNase-Free distilled water to a concentration of 2 μg/μL in a total volume of 11 μL and were electroporated with a Neon® Nucleofector using a 100 μL Neon® Transfection Kit (all Thermo Fisher Scientific, Waltham, MA) with 1700 V and one pulse of 20 ms. Seven to eight transfections per cell line were performed and subsequently pooled in a 500 mL shake flask with a 200 mL working volume. Supernatants were harvested five days post transfection by centrifugation (170 g, 10 min) and were sterile-filtered before further use.

Insect cells: Tnms42, an alphanodavirus-free subclone of the High-Five insect cell line [17,18], were routinely propagated in adherent culture in HyClone SFM4 insect cell medium (Cytiva, Marlborough, MA) at 27 °C and were expanded in suspension culture for recombinant protein expression. A passage one virus seed stock expressing the SARS CoV-2 RBD was amplified in *Sf*9 cells to generate a passage three working stock and was titrated by plaque assay as previously described [19]. *Tnms*42 insect cells at 2×10^6 cells/mL were infected at a multiplicity of infection (MOI) of two, and the supernatant was harvested three days post-infection, clarified (1000 g, 10 min, followed by 10,000 g, 30 min) and was filtered through a 0.45 μm filter before downstream procedures.

Tobacco plants: The pEAQ-HT-RBD expression vector was transformed into *Agrobacterium tumefaciens* strain UIA143 [6]. Syringe-mediated agroinfiltration of leaves from five-week-old *Nicotiana benthamiana* ΔXT/FT plants was used for transient expression [20]. Four days after infiltration, leaves were harvested and intracellular fluid was collected by low-speed centrifugation as described in detail elsewhere [21].

E. coli: The pET30a*cer*-CASPON—NP expression vector was transformed into *E. coli* enGenes-X-press for growth-decoupled recombinant protein production as described elsewhere [7]. Briefly, for cultivation cells were grown in fed-batch mode in a 1.0 L (0.5 L batch volume, 0.5 L feed) DASGIP® Parallel Bioreactor System (Eppendorf AG, Hamburg, DE) equipped with standard probes (pH, dissolved oxygen [pDO]). The pH was maintained at 7.0 $\pm$ 0.05, temperature was maintained at 37 $\pm$ 0.5 °C during the batch phase and decreased to 30 $\pm$ 0.5 °C at the beginning of the feed phase. The dissolved oxygen level was stabilized at > 30% (V/V). Induction of NP production was facilitated at feed hour 19 with the addition of 0.1 mM IPTG and 100 mM arabinose.

2.1.4. Downstream procedures

Purification of SARS-CoV-2 RBD and tRBD from different expression systems: His-tagged RBD and tRBD from filtered HEK supernatants, as well as RBD from *Tnms*42 insect cell supernatants, were concentrated and diafiltrated against 20 mM sodium phosphate buffer supplemented with 500 mM NaCl and 20 mM imidazole (pH 7.4) using a Labscale TFF system equipped with a Pellicon™ XL Ultracel 5 kDa, 0.005 m^2 ultrafiltration module (Merck, Darmstadt, DE). The proteins were captured using a 5-mL HisTrap FF Crude or a 1-mL HisTrap Excel immobilized metal affinity chromatography (IMAC) column connected to an ÄKTA Pure chromatography system (all from Cytiva, Marlborough, MA) and were eluted by applying a linear gradient of 20 to 500 mM imidazole over 5 to 20 column volumes, as appropriate. Intracellular fluid collected from plant material was directly loaded onto a 5-mL HisTrap HP column and was purified as described elsewhere [22]. CHO-K1 and CHO-S expression supernatants were supplemented with 20 mM imidazole and were directly loaded onto a 1-mL HisTrap FF column connected to an ÄKTA Start

chromatography system (both Cytiva, Marlborough, MA), equilibrated with 50 mM sodium phosphate buffer supplemented with 300 mM NaCl and 20 mM imidazole (pH 7.4). Proteins were eluted by applying a linear gradient of 20 to 500 mM imidazole over 20 column volumes.

Fractions containing RBD or tRBD were pooled and either diluted with 20 mM sodium phosphate buffer (pH 7.4) to a conductivity of ~10 mS/cm and then loaded onto a Fractogel EMD DEAE column (Merck Millipore, Germany) or loaded onto HiTrap DEAE FF column (Cytiva, Marlborough, MA), both pre-equilibrated with 20 mM sodium phosphate buffer (pH 7.4). A residence time of two minutes was used. The flow-through fractions, containing RBD or tRBD, were collected. Impurities were subsequently eluted using 20 mM sodium phosphate buffer, 1 M NaCl, pH 7.4 and the column was cleaned in place by incubation in 0.5 M NaOH for 30 min. The protein of interest present in the flow-through fraction was buffer-exchanged into PBS using Amicon Ultra-15 Ultracel 10 kDa spin columns (Merck Millipore, Germany) or was dialyzed against PBS. IMAC-captured RBD from insect cell supernatants was ultra- and diafiltrated using Amicon Ultra Centrifugal Filter Units (10 kDa MWCO, Merck Millipore) to change the buffer to PBS and was further purified by size exclusion chromatography using a HiLoad 16/600 Superdex 200 pg column (Cytiva, Marlborough, MA) equilibrated with the same buffer. Fractions containing RBD were concentrated using Amicon Ultra-15 Ultracel 10 kDa spin columns (Merck Millipore, Germany). All purified proteins were quantified by measuring their absorbance at A_{280} with a Nanodrop instrument and stored at -80 °C until further use.

Purification of SARS-CoV-2 NP from E. coli cellular lysates: The purification of NP was optimised and performed as described by De Vos and colleagues [10]. In brief, NP was produced by using the CASPON platform process [9] with modifications. The process consisted of an IMAC capture step (WorkBeads 40 Ni NTA, Bio-Works, Uppsala, SE) of the clarified cell lysate. A nuclease treatment (Salt Active Nuclease High Quality, ArcticZymes Technologies ASA, Tromsø, NO) was required to reduce CASPON—NP nucleic acid binding. Imidazole was removed from the IMAC eluate using a Butyl Sepharose HP hydrophobic interaction chromatography (Cytiva, Uppsala, SE) which also separated full-length from fragmented CASPON—NP. A variant of cpCasp2 [8] was used to remove the affinity fusion-tag. Finally, an IMAC polishing step was used to separate native NP from residual CASPON—NP, the free affinity fusion-tag, the affinity-tagged cpCasp2 variant and metal binding host cell proteins. The polishing fraction was buffer exchanged to PBS using tangential flow filtration on Pellicon 3 Ultracel 10 kDa membrane (Merck Millipore, Darmstadt, DE).

Purification of mAb CR3022: mAb CR3022 was purified by affinity chromatography using a 5-mL HiTrap Protein A HP column connected to an ÄKTA pure chromatography system (both from Cytiva, Marlborough, MA) according to the manufacturer's protocol. The antibody was eluted using 0.1 M glycine-HCl buffer (pH 3.5). Eluate fractions containing CR3022 were immediately neutralized using 1 M Tris−HCl buffer (pH 8.0), pooled and concentrated using Amicon ultrafiltration cartridges with a cut-off of 10 kDa (Merck, Darmstadt, DE) and were further dialyzed against PBS (pH 7.4) at 4 °C overnight using Snake-Skin Dialysis Tubing with a 10 kDa cut-off (Thermo Fisher Scientific, Germering, DE). CR3022 was further purified by size exclusion chromatography using a HiLoad 16/600 Superdex 200 pg column (Cytiva, Marlborough, MA) equilibrated with the same buffer as used for dialysis.

2.2. Commercial antigen and antibody reagents

Recombinant spike proteins of the four common-cold hCoV strains, HKU-1, OC43, NL63 and 229E were purchased from Sino Biological Inc, Beijing, CN (#40,606-V08B, #40,607-V08B, #40,604-V08B and #40,605-V08B, respectively). A recombinant chimeric human/mouse anti-SARS-CoV-2 NP antibody consisting of a mouse scFv

fused to the Fc region of human IgG1 (clone 1A6) was purchased from Abcam, Cambridge, UK (#ab272852).

2.3. Assessment of recombinant protein quality

2.3.1. Analytical size exclusion chromatography (SEC)

High-performance liquid chromatography (HP)-SEC experiments were performed on a Dionex^{TM} UltiMate^{TM} 3000 RSLC system equipped with an LPG-3400SD Standard Quaternary Pump module, a WPS-3000 TSL Analytical Split-Loop Well Plate Autosampler and a DAD-3000 Diode Array Detector equipped with a ten μL analytical flow cell (all from Thermo Fisher Scientific, Germering, DE). RBD, tRBD and NP samples (25−80 μg per sample) were run on a Superdex^{TM} 200 Increase 10/300 GL column (Cytiva, Uppsala, SE) and UV signals were detected at λ = 280 nm. For RBD and tRBD, Dulbecco's PBS buffer (DPBS) supplemented with 200 mM NaCl was used as mobile phase, the flow rate was set to 0.75 mL/min and a 45 min isocratic elution was performed. For NP samples 0.1 M sodium phosphate buffer (pH 7.0) containing 300 mM NaCl was used as mobile phase, the flow rate was set to 0.5 mL/min and a 60 min isocratic elution was performed. HP control, data acquisition and data evaluation were performed using Chromeleon^{TM} 7.2 Chromatography Data System software (Thermo Fisher Scientific, Germering, DE). Sample purity (P), monomer (M), dimer (D) and full-length (FL) content were determined based on the respective peak area of the UV signal at 280 nm. For RBD and tRBD purity was defined as P=(M+D)/total area, monomer and dimer content were respectively defined as M[%]=M/(M+D)*100 and D=100-M[%]. For NP, full-length content was defined as FL[%]=FL/total area.

2.3.2. Bio-layer interferometry (BLI) measurements

Interaction studies of RBD, tRBD and NP with in-house produced anti-RBD mAb CR3022 and a commercial anti-SARS-CoV-2 nucleocapsid protein antibody (ab272852, Abcam, Cambridge, UK) were performed on an Octet RED96e system using high precision streptavidin (SAX) biosensors (both from FortéBio, Fremont, CA). Antibodies were biotinylated using the EZ-Link Sulfo-NHS-LC-Biotin kit (Thermo Fisher Scientific, Waltham, MA). Excess sulfo-NHS-LC-biotin was quenched by adding Tris−HCl buffer (800 mM, pH 7.4) to a final concentration of 3 mM. Biotinylated antibodies were further purified using PD-10 desalting columns (Cytiva, Marlborough, MA) according to the manufacturer's protocol. All binding assays were conducted in PBS supplemented with 0.05% (v/v) Tween 20 and 0.1% (w/V) BSA (PBST-BSA) at 25 °C with the plate shaking at 1000 rpm. SAX biosensors were first equilibrated in PBST-BSA and then loaded with the respective biotinylated capture molecules, either for 180 s (34 nM CR3022 solution) or until a signal threshold of 0.8 nm was reached (50 nM anti-NP mAb solution). Subsequently, antibody-loaded biosensors were dipped into PBST-BSA for 90 s to record a baseline, before they were submerged into different concentrations of their respective analytes. To determine K_D values, biotinylated antibodies loaded onto biosensors were exposed to six concentrations of the binding partners (RBD, tRBD or NP) to cover a broad concentration range around the respective K_D value [23]. For antigen association, mAb CR3022 was exposed to a three-fold serial dilution of RBD or tRBD (range: 300 nM−1.2 nM in PBST-BSA) for 300 s, while anti-NP mAb-was dipped into two-fold serial dilutions of the NP protein (40 nM - 1.3 nM in PBST-BSA) for 600 s. For dissociation, the biosensors were dipped into PBST-BSA. Each experiment included a baseline measurement using PBST-BSA (negative control) as well as a positive control (RBD monomer) where applicable. SAX biosensors loaded with biotinylated CR3022 or anti-NP mAb could be regenerated by dipping them into 100 mM glycine buffer (pH 2.5). RBD or tRBD proteins were measured in triplicates or quadruplicates, while NP proteins were measured in duplicates. No unspecific binding of proteins to SAX biosensors was observed. Data were evaluated under

consideration of the lower limit of detection (LLOD) and lower limit of quantification (LLOQ) as reported elsewhere [24,25]. The analysis was performed using the Octet data analysis software version 11.1.1.39 (FortéBio, Fremont, CA) according to the manufacturer's guidelines. For easier comparison of the RBD variants produced in different expression hosts, the K_D values were determined from the measured equilibrium response (steady state analysis). However, the interaction between the CR3022 mAb and the final tRBD batches were also evaluated kinetically by fitting the BLI data to a 2:1 heterogeneous ligand binding model. Note, although the CR3022 mAb has two identical binding sites, the second binding event is dependent on the first binding since allosteric effects or sterical hindrance can ultimately lead to a positive or negative cooperative binding behaviour [16,26,27]. However, in case of the reported interaction, the affinity constant (K_D) values are very close to one other in the low nanomolar range.

The interaction between the NP protein and the anti-NP mAb is difficult to characterise due to avidity effects that arise from the dimeric nature of both interaction partners. Kinetic evaluation of the BLI data is problematic since the dissociation curves are heterogenic. Additionally, if the dissociation phase shows less than 5% decrease in signal during the defined dissociation phase, as observed for the lower concentration range of NP protein, a precise determination of the dissociation rate constants (k_d) is not possible [28,29]. However, it is feasible to calculate an upper limit for the k_d (s^{-1}) which is given by $k_d < -\ln(0.95)/t_d$, where td is the dissociation time in seconds [28,30] Thus, an upper limit for the K_D value, calculated by the ratio of kd/ka, resulted in < 0.7 nM, suggesting a strong interaction in the picomolar range. Moreover, for comparison of single batches the observed binding rate (k_{obs}) was plotted as a function of the NP concentration and used for the comparison of the single batches.

2.3.3. Liquid chromatography electrospray ionization mass spectrometry (LC/ESI-MS)

Purified proteins were S-alkylated with iodoacetamide and digested with endoproteinases LysC (Roche, Basel, CH) and GluC (Promega, Madison, WI) or chymotrypsin (Roche, Basel, CH) in solution. Digested samples were analyzed using a Thermo Ultimate 3000 HP connected to a 150 × 0.32 mm, 5 μm BioBasic C18 column (both Thermo Fisher Scientific, Waltham, MA) and a maXis 4 G QTOF mass spectrometer (Bruker, Billerica, MA). An 80 mM ammonium format buffer was used as the aqueous solvent and a linear gradient from 5% B (B: 80% acetonitrile) to 40% B in 45 min at a flow rate of 6 μL/min was applied, followed by a 15 min gradient from 40% B to 95% B that facilitated elution of large peptides. The MS system was equipped with the standard ESI source and operated in positive ion, DDA mode (= switching to MSMS mode for eluting peaks). MS-scans were recorded (range: 150−2200 Da) and the six highest peaks were selected for fragmentation. Instrument calibration was performed using ESI calibration mixture (Agilent, Santa Clara, CA). The analysis files were converted (using Data Analysis, Bruker) to mgf files, which are suitable for performing a MS/MS ion search with MASCOT. The files were searched against a database containing the target sequences. In addition, manual glycopeptide searches were done. Glycopeptides were identified as sets of peaks consisting of the peptide moiety and the attached N-glycan varying in the number of HexNAc, hexose, deoxyhexose and pentose residues. Theoretical masses of these peptides were determined using the monoisotopic masses for the respective amino acids and monosaccharides.

2.4. Ethics statement

The present study includes work with human sera from three different sites. Acute lithium heparin plasma samples collected from outpatient and hospitalised individuals for routine clinical testing were available at the B&S Central Laboratory Linz, Austria. Left-over

samples were assessed for SARS-CoV-2 antibody levels and neutralizing titers in the early phase of infection. The study protocol and the use of residual material from routine clinical examinations for biomedical research without explicit consent was approved by the ethics committee of Upper Austria (EK1083/2020), in accordance with the Declaration of Helsinki. For ELISA validations, left-over sera from SARS-CoV-2 patients and sera from convalescent donors, as well as historical sera (collected prior to 2020) were taken from the MedUni Wien Biobank, as approved by the ethics committee of the Medical University of Vienna (EK 1424/2020). All individuals whose samples were used provided written informed consent for their samples to be added to a biobank and to be used for biomedical research/methods evaluation. The inclusion of residual material from routine clinical examinations without explicit consent was approved by the Ethics Committee of the Medical University of Vienna. The underlying sample collections were reviewed and approved by the ethics committee of the Medical University of Vienna (EK 595/2005, EK 404/2011, EK 518/2011), or by the ethics committee of the City of Vienna (EK-11−117−0711), respectively. Samples from hospitalised COVID-19 patients at the University Hospital of Innsbruck, reconvalescent COVID-19 patients with persistent cardio-pulmonary damage participating in a prospective observational study (CovILD-study, ClinicalTrials.gov number, NCT04416100, Reference: PMID: 33303539) and reconvalescent persons volunteering as plasma donors were used for test validation in Innsbruck [31]. The underlying sample collections were reviewed and approved by the ethics committee of the Medical University of Innsbruck (EK 1103/2020, EK 1167/2020). Left-over SARS-CoV-2 acute and convalescent sera from blood donors and pre-COVID-19 sera from the Austrian Institute of Technology were taken for SARS-CoV-2 antigen pre-validation. The study protocol and the use of residual material from routine clinical examinations for biomedical research/methods evaluation without explicit consent was approved by the ethics committee of the city of Vienna (EK 20−179−0820).

2.5. Human serum and plasma samples

Careful consideration of samples size is important to ensure that a study has sufficient participants to be meaningful and to also accurately detect small effects. Sample size requirements usually rely on hypothesized values on sensitivity and specificity and their clinically acceptable degree of precision, and an estimated prevalence of disease in the target population [32]. At the time of clinical validation we had data on the estimated 5% seroprevalence in Austria [33] as well as data on specificity and sensitivity estimates from a previous study on SARS-CoV-2 diagnostic tests available [34]. Sample size estimations were based on the following assumptions: Type I error 0.05 (two-sided), type II error 0.20. At the beginning of the pandemic, high specificity was required to ensure a sufficient positive predictive values (PPV) at a low seroprevalence of about 5%. Thus, it was necessary to determine the specificity with high accuracy. To discriminate a specificity of 99.2% (see, e.g. Abbott SARS-CoV-2 IgG, [34]) from one that is 1% below this value (H0=98.2%), a total of 1.126 negative cases would be required, just as many as have been included in the specificity cohort. In a real-life setting, sensitivities of Anti-SARS-CoV-2 immunoassays are usually in the range of 90% [31,34]. To significantly differentiate a sensitivity of 95% from 90%, at least 239 positive samples would need to be included (244 samples were used in the sensitivity cohort).

2.5.1. Sensitivity cohorts

SARS-CoV-2 acute sera from a cohort of outpatient and hospitalised individuals, B&S central laboratory Linz, Austria: A cohort of hospitalised individuals and outpatients included a total number of 64 SARS-CoV-2 RT-PCR-confirmed (from respiratory specimens) COVID-19 patients (median age 65 [14−95, IQR 56−87 years], 17.2% females)

who were treated in one of the two tertiary care hospitals Konventhospital Barmherzige Brueder Linz or Ordensklinikum Linz Barmherzige Schwestern in Linz, Austria, between March 15th and April 10th 2020. Of these, ten patients were treated as outpatients and 54 patients were hospitalised; twelve of them were treated at the intensive care unit (ICU). From the 64 patients, a total of 104 serial blood samples were drawn at different time points after symptom onset until April 10th, 2020. Sixty-four patients had at least one, 28 patients had two, nine patients had three and three patients had four blood draws, which were sent to the central laboratory for routine clinical testing. The date of onset of symptoms was retrieved from medical records and was available for all patients. Left-over lithium heparin plasma samples were aliquoted and frozen at −80 °C and had up to two freeze-thaw cycles.

Sera of SARS-CoV-2-positive patients and convalescent donors, Medical University of Vienna and Medical University of Innsbruck: The SARS-CoV-2 positive samples for ELISA validation comprise 70 serum specimens from unique patients or convalescent donors with (previous) SARS-CoV-2 infection from Vienna (either PCR-positive or symptomatic close contacts), as well as 174 SARS-CoV-2 PCR positive patients including hospitalised patients (n = 123) and convalescent blood donors (n = 51) from Innsbruck. All samples were collected >14 days after symptom onset (or positive PCR, in case of asymptomatic infection). A representative serum panel of these samples (n = 28−31) was taken for the pre-validation of SARS-CoV-2 antigens by ELISA and for the assessment of SARS-CoV-2 neutralization titers.

SARS-CoV-2-convalescent and acute sera from a cohort of non-hospitalised blood donors, Austrian Institute of Technology (AIT) and Medical University of Vienna: The sensitivity cohort for antigen pre-validation covered 124 COVID sera. Among these, 96 sera were deidentified excess samples from infected individuals collected for routine SARS-CoV-2 serodiagnosis using a seven-plex bead-based Luminex-FlexMap system-based serotest and were available at the AIT. These serotests had been conducted similar to the analysis procedure outlined below. Seronegativity and/or seropositivity was based on cutoff values and end-point titres defined according to Frey et al. [35] on the basis of 160 pre-COVID-19 sera. Additionally, the study cohort included a set of 28 COVID-19 sera from the Medical University (from the above), covering samples from primarily asymptomatic individuals or those with mild to moderate illness.

2.5.2. Specificity cohorts

Pre-COVID-19 cohort, Meduni Wien Biobank: The pre-COVID-19 cohort covered a total of 1126 samples from healthy, non-SARS-CoV-2-infected individuals collected before 2020 to guarantee seronegativity. Banked human samples including sera from voluntary donors (n = 265, median age 38 [25−52] years, 59.0% females), samples from a large population-based cohort aged 8−80 years, representing a cross-section of the Austrian population (N = 494, collected 2012−2016 from November to March to increase the likelihood of infection with other respiratory viruses, median age 43 [26−56], 50.0% females) [36], samples from patients with rheumatic diseases (N = 359, median age 52 [41-61], 76.0% females), and eight samples from patients with previous seasonal coronavirus infection collected for routine clinical testing at the Regional Hospital Feldkirch. Sera with PCR-confirmed hCoV infection (hCoV 229-E, n = 3; hCoV NL63, n = 2 [one of which with 229E co-infection], hCoV OC43, n = 2; non-typed, n = 2) were drawn between January 2019 and February 2020 and were kindly provided by Andreas Leiherer (Vorarlberg Institute for Vascular Investigation and Treatment VIVIT, Dornbirn, AT). A set of 14 sera of the above (not including hCoV sera) was used for pre-validation of SARS-CoV-2 antigens in an ELISA. Samples (except for those from patients after seasonal .coronavirus infection) were processed and stored according to standard operating procedures within the MedUni Wien Biobank facility in a certified (ISO 9001:2015) environment [37].

Pre-COVID cohort, Austrian Institute of Technology: Control sera from AIT covered 210 samples of blood donors were obtained in 2014 from the Austrian Red Cross blood bank; collected samples have been stored at −80 °C without any freeze thaw cycles.

2.6. Pre-validation of antigens using seroreactivity assays

2.6.1. Luminex assay

In-house produced SARS-CoV-2 RBD, tRBD and NP as well as spike proteins of hCoV HKU-1, OC43, NL63 and 229E (all from Sino Biological Inc, Beijing, CN) were separately coupled to MagPlex carboxylated polystyrene microspheres (Luminex Corporation, Austin, TX) according to the manufacturer's instruction, with the following minor modifications: For coupling, five μg of each antigen was used per one million microspheres. Coupling was performed in a total volume of 500 μL in 96-Well Protein LoBind Deepwell plates (Eppendorf, Hamburg, DE) and plates were incubated at 600 rpm on a Heidolph Titramax 1000 plate shaker (Heidolph, Schwabach, DE). After each incubation step plates were centrifuged at 400 g for one minute. To collect the microspheres at the bottom of the plate, plates were placed on a Magnetic plate separator (Luminex Corporation, Austin, TX) and the supernatant was poured off by inverting the plates. Coupling was performed in 200 μL coupling buffer (50 mM MES, pH 5.0). Microspheres with coupled proteins were stored in Assay buffer (PBS supplemented with 1% (w/V) BSA, 0.05% (w/V) NaN$_3$, pH 7.4) at a final concentration of 10,000 microspheres per μL at 4 °C in the dark. Sera of patients and controls were five-fold diluted in PBS-Triton X-100 buffer (PBS supplemented with 1% (V/V) Triton X-100, 0.05% (w/V) NaN$_3$, pH 7.4) and were further diluted 240-fold with Assay buffer. Coupled microspheres (800 beads per sample) were first equilibrated to room temperature for 30 min. Plates were then vortexed for 30 s and sonicated for 20 s using a Transsonic T470/H sonicator (Elma Electronics, Wetzikon, CH). The required amounts (based on multiples of samples to be analysed) of microspheres (+10% excess) were transferred to 1.5 mL Protein LoBind tubes (Eppendorf, Hamburg, DE) and centrifuged for three minutes at 1200 g. Microtubes were then placed on a Magneto Dynal magnetic tube separator (Invitrogen, Carlsbad, CA), supernatants were carefully removed and microspheres were resuspended in 200 μL Assay buffer. Different microspheres were then combined in a 50 mL Falcon tube to yield a total of 800 microspheres per coupled antigen in 30 μL assay buffer per single measurement. Thirty μL of the mixed microsphere suspension was then transferred to wells of a clear 96-well microplate (Corning Inc, Corning, NY). Assay plates were placed on the magnetic plate separator and supernatants were poured off by inverting the plates. Fifty μL of sera (1:1200-diluted) or assay buffer (blank samples) was applied to each well. Assays were incubated for two hours at RT on the plate shaker (600 rpm). Assay plates were placed on the magnetic plate holder and the supernatants were poured off by inverting the plates. Microspheres were washed by removing the magnetic plate holder and the addition of 100 μL Wash buffer (PBS; 0.05% (V/V) Tween-20; 0.05% (w/V) NaN$_3$; pH 7.4) per well. After two minutes of incubation at room temperature, plates were again placed on the magnetic plate holder and supernatants were poured off. After three wash steps 50 μL of a 1:1 mixture of 2.5 μg/mL goat anti-human R-Phyco AffiniPure F(ab')$_2$, Fcγ-specific (Jackson ImmunoResearch Labs Cat# 109−116−098, RRID:AB_2,337,678)and F(ab')$_2$-specific IgG (Jackson ImmunoResearch Labs Cat# 109−116−097, RRID: AB_2,337,677) in Assay buffer were added. Plates were incubated for one hour at room temperature on the plate shaker (600 rpm) in the dark. Microspheres were then washed again three times and microspheres were resuspended in 100 μL Assay buffer and median fluorescence intensity (MFI) was immediately measured on a Flexmap 3D Suspension Array System (BioRad, Hercules, CA) with a minimal Count of 100 per microsphere type, a DD Gating of 7500−25,000 and the Reporter Gain set to "Enhanced PMT (high)". MFI values were extracted from FM3D result files. A minimum microsphere count of 25 counts was set as cut-off. All samples and single bead types analysed fulfilled the minimum bead count criterium. FM3D results files were compiled in Microsoft Excel and were log2-transformed and blank-corrected by subtracting the mean MFI values of blank samples (assay buffer only) from MFI values of the test samples.

2.6.2. ELISA assay

Initially, ELISA conditions were optimised in terms of antigen coating conditions (0.5−8 μg/mL) and serum-dilutions (1:50−1:3200) to optimise the trade-off between background seroreactivity and sensitivity in samples from individuals with weak antibody responses. The final protocol was as follows: SARS CoV-2 and hCoV antigens (see above) were diluted to 6 μg/mL in phosphate-buffered saline (PAN Biotech #P-04−36,500) and 50 μL were added to each well of MaxiSorp 96-well plates (Thermo #442,404). After incubation at 4 °C overnight, wells were washed 3x with PBS + 0.1% Tween-20 (PBS-T, Merck #8.22184) and blocked for one hour at room temperature with PBS-*T* + 3% (w/V) milk powder (Fluka #70,166). Serum samples were diluted 1:200 in PBS-*T* + 1% (w/V) milk powder. 100 μL were applied to each well and plates were incubated for two hours at RT with shaking (450 rpm). Plates were washed 4x before incubation with goat anti-human IgG (Fc-specific) horseradish peroxidase (HRP) conjugated antibodies (Sigma-Aldrich #A0170, RRID:AB_257,868; 1:50,000 in PBS-*T* + 1% (w/V) milk powder, 50 μL/well) for one hour at RT while shaking. After four washes, freshly prepared substrate solution (substrate buffer [10 mM sodium acetate in dH$_2$O, pH 5, adjusted with citric acid] + 1:60 TMB-stock [0.4% Tetramethylbenzidine (Fluka #87,748) in DMSO] + 1:300 H$_2$O$_2$ [0.6% in dH$_2$O]) was applied (150 μL/well) and plates were incubated for 25 min at RT with shaking. Reactions were stopped by the addition of 1 M sulfuric acid (25 μL/well). Absorbance was measured at 450 nm on a Tecan Sunrise Microplate reader using a reference wavelength of 620 nm and the Magellan V 7.2 SP1 Software.

2.7. TECHNOZYM anti-SARS-CoV-2 RBD and NP IgG ELISAs assays

The above-described methodology was slightly adapted for the development of the TECHNOZYM Anti SARS-CoV-2 NP and RBD IgG ELISA test kits (Technoclone, Vienna, AT). The tests plates were provided with the antigens coated at a concentration of 6 μg/mL and lyophilized according to a proprietary in-house protocol. The RBD test kit employs the described tRBD as coating antigen. To allow for a quantitative measurement of SARS-CoV-2 antibody levels, a calibrator set consisting of five calibrators with assigned values was provided for the creation of a calibration curve and was run in parallel with the patients' samples. The calibrated values were established using the monoclonal antibody CR3022 as a reference material, with 1 U equivalent to 100 ng/mL mAb CR3022 (#Ab01680−10.0, Absolute Antibody, Oxford, UK). The calibrator set covered the concentration range 0 − 100 U/mL and concentrations of anti SARS-CoV-2 IgG antibodies recognizing either tRBD or NP in patient sera could be read directly from the calibration curve.

2.8. Technozym NP and RBD IgG ELISA test validations

The established NP and RBD IgG ELISA assays were either processed manually and analyzed on a Filtermax F5 plate reader (Molecular Devices, San José, USA) or on an Immunomat instrument (Serion Diagnostics, Würzburg, DE) according to the manufacturer's instructions. IgG antibody levels were reported as numeric values in form of arbitrary U/mL derived from the five-point calibration curve. Cut-offs for test validations were determined by ROC-analysis and the non-parametric 99th right-sided percentile method (CLSI C28-A3). Sensitivities, specificities, PPV, and negative predictive values (NPV, both at 5% estimated seroprevalence) were calculated. ROC-analysis data

from automated tests (including Abbott ARCHITECT SARS-CoV-2 IgG, DiaSorin LIAISON® Anti-SARS-CoV-2 S1/S2 IgG) were available for 64 of the positive and 1117 of the negative samples from a previously published study [34].

2.9. SARS-CoV-2 neutralisation assay

A tissue culture infectious dose (TCID$_{50}$) assay for authentic SARS-CoV-2 virus was developed for the determination of neutralizing antibodies. The virus was originally isolated from a clinical specimen, a nasopharyngeal swab taken in mid-March 2020 from a 25-year old male patient in Lower Austria, and was further passaged twice on Vero E6 TMPRSS-2 cells in Dulbecco's modified Eagle's medium (DMEM) with 10% (V/V) foetal bovine serum (FBS). Vero E6 TMPRSS-2 cells, initially described in Hoffmann et al. [38] were kindly provided by Stefan Pöhlmann; Deutsches Primatenzentrum, Göttingen, Germany.

Briefly, assays were performed with Vero 76 clone E6 cells (CCLV-RIE929, Friedrich-Loeffler-Institute, Riems, Germany) cultured in minimum essential medium Eagle (E-MEM) with BioWhittaker Hank's balanced salt solution (HBSS) (Lonza, Basel, CH) supplemented with 10% (V/V) FBS (Corning Inc, Corning, NY). Neutralizing antibody titres in human serum and plasma were determined as previously described [39] with the following alterations: the heat-treated sera were diluted 1:4 in triplicates in serum-free HEPES-buffered DMEM medium. In the case neutralizing antibody titres were determined in human lithium heparin plasma, no heat-treatment was applied and the medium was supplemented with 1x Antibiotic/Antimycotic solution (Thermo Fisher Scientific, Waltham, MA). The heat treatment had no effect on neutralizing titres, as verified in a pre-experiment on SARS-CoV-2 positive and negative plasma samples. In addition, a toxicity control, which was processed the same way as plasma samples, was included. Here, no virus was added, to prevent a false readout of the assay. Cytopathic effect (CPE) was evaluated and scored for each well using an inverted optical microscope. To determine neutralization titres the reciprocal of the highest serum dilution that protected more than 50% of the cells from the CPE was used and was calculated according to Reed and Muench [40].

2.10. Statistical analyses

Raw data were assessed for normality of distribution and homogeneity of variances using the D'Agostino−Pearson omnibus test before statistical procedures. Differences in median seroreactivity between pre-COVID and COVID sera were compared using the Mann-Whitney U tests on blank-corrected log2-transformed median fluorescence intensities (Luminex data) or OD$_{450}$ absorbances (ELISA), respectively. Correlation analyses of nonparametric data were performed by Spearman's rank-order correlation (r_s), otherwise Pearson's' correlation (r) was used. Relative IgG signals of outliers against SARS-CoV-2 and hCoV antigens were compared by One-Way ANOVA followed by a Sidak test to correct for multiple comparisons. ROC-analysis data from automated tests were compared to the established ELISA tests according to DeLong. Sensitivities and specificities were compared by z-tests. Data on the diagnostic performances of antigens and cross-reactivity were analysed using Graphpad Prism Version 8.1.0 (GraphPad Software, San Diego, CA, USA) Validation data were analysed using MedCalc v19 (MedCalc Software, Ostend, Belgium) and analyse-it 5.66 (analyse-it Software, Leeds, UK) and SPSS 23.0 (SPSS Inc.). Data from SARS-CoV-2 acute sera from hospitalised individuals or outpatients obtained by the B&S Central Laboratory Linz were statistically analysed with the MedCalc 13.1.2.0.

2.11. Role of the funding source

The funding sources had no role in the study design, the collection, analysis and interpretation of data, in writing this manuscript and in the decision to submit the paper for publication.

3. Results

3.1. Comparative profiling of expression hosts for SARS CoV-2 RBD and NP production for diagnostic use

Initially, five eukaryotic expression systems were compared for their capacity to support high-quantity and high-quality expression of the glycosylated SARS-CoV-2 spike RBD. Our pre-defined quality attributes covered activity in a functional binding assay using a conformation-dependent RBD-specific antibody (CR3022), protein integrity and glycosylation determined by mass spectrometry, as well as manufacturability (**Fig. 1a**). Biolayer interferometry analysis revealed that RBD obtained from different mammalian and insect expression systems have comparable affinities (range: 21 − 43 nM) for the mAb CR3022 (**Fig. 1a, left panel**). Glycan analysis confirmed host-specific N-glycosylation of the respective proteins, which was of complex-type for the human (HEK-6E) and non-human mammalian cell lines (CHO-K1, CHO-S) as well as for plant (*Nicotiana benthamiana*)-derived RBD. We found paucimannosidic N-glycosylation for the *Trichoplusia ni* insect cell line (*Tnms*42)-derived RBD (**Fig. S1a, b**). Peptide mapping verified the integrity of the protein primary structure (data not shown). Unoptimised and small-scale electroporation of non-human cell lines (CHO-K1 and CHO-S) and baculovirus infection of insect cell lines (*Tnms*42) produced overall yields after purification of less than one mg RBD per litre of culture. Polyethylenimine (PEI) transfection of HEK cells readily provided higher overall volumetric yields (~40 mg/L) without further process optimisation (**Fig. 1a, left panel**). Analytical size-exclusion chromatography (HP-SEC) revealed expression platform and production batch-dependent RBD homo-dimer contents. (**Fig. S2**). For plant-expressed RBD, dimerisation was particularly pronounced. We identified an unpaired cysteine residue (Cys538) close to the C-terminus of the canonical RBD sequence as a possible cause for RBD dimerisation. A truncated RBD construct (tRBD) lacking this cysteine residue was less prone to homodimer formation, but retained full functionality in the binding assay and similar expression yields (**Fig. 1a right panel, Fig. S3**). From a manufacturing perspective, tRBD thus provided less batch-to-batch variation, which is a pre-requisite for a diagnostic antigen.

To assess the performance of the antigens for discrimination between sera from SARS-CoV-2-exposed (*n* = 124) and uninfected individuals (*n* = 210), we applied a high-throughput (HTP) automated bead-based multiplex assay (**Fig. 1b, c**). The performance of diagnostic tests is commonly assessed through receiver operating characteristic (ROC) curves and the analysis of area under the ROC curve (AUC-ROC). ROC curves are simple graphical representations of the relationship between sensitivity and specificity of a test over all possible diagnostic cut-off values and AUCs give the overall ability of a test to discriminate between two populations [41]. We used theses analyses to assess potential differences in the diagnostic performance of the RBD from different expression hosts. Almost all antigens at this high purity demonstrated AUC values of >0.99, demonstrating the high suitability of the RBD from any source as diagnostic antigen. The AUC value of insect-derived RBD was slightly lower (AUC: 0.978 [0.964−0.992]); the differences, however, were not significant (**Fig. 1b**). We then applied antigen-specific cut-offs to compare the performance of the antigens at a pre-defined consensus specificity of 99.1%. At this criterion, we obtained high sensitivities (range 94.4%−96.0%) with all antigens, except for insect-derived RBD. There, seroreactivity with pre-COVID-19 sera was about 2^2- (4)-fold higher than observed for CHO-expressed RBDs. This resulted in 26% of COVID-19 sera to fall below the threshold, increasing the rate of false-negatives (**Fig. 1c**). The tRBD displayed a comparable seroreactivity profile to the RBD.

During our pre-validation experiments we observed a strong effect of residual host cell proteins on assay performance (**Fig. S4**), even in formulations derived from human cell lines. Therefore, RBD/
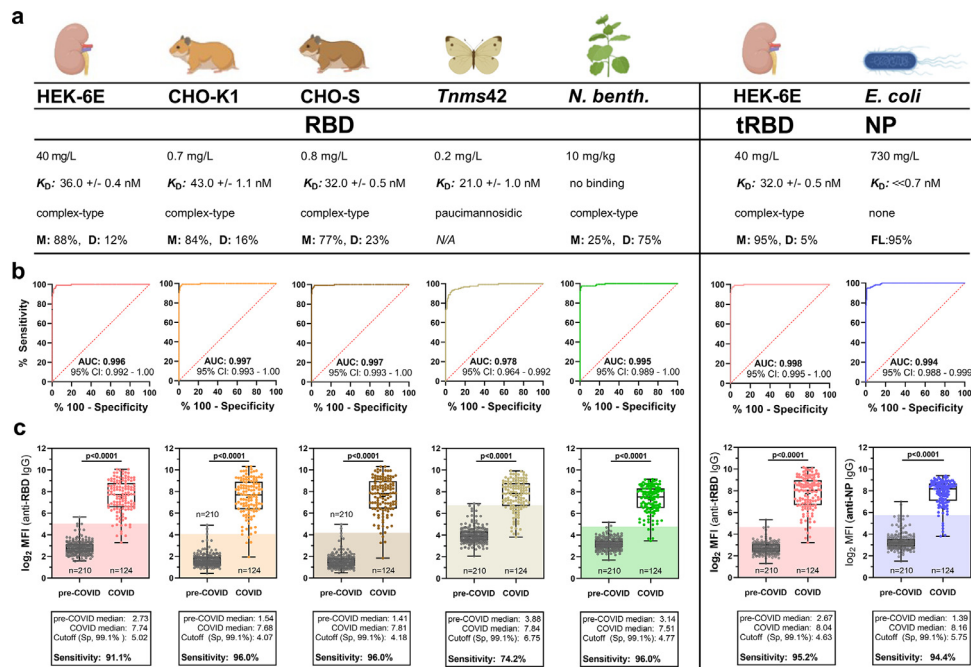
Fig. 1. Comparative profiling of SARS CoV-2 antigens from different expression hosts for serodiagnosis. a-c, the canonical SARS-CoV-2 RBD expressed in five biotechnological platforms (HEK-6E, CHO-K1, CHO-S, *Tnms*42, *N. benthamiana,* **left panel**), an optimised RBD construct expressed in HEK cells (tRBD) as well as the NP produced in *E. coli* (**right panel**) were compared in terms of biotechnological parameters as well as seroreactivity to identify ideal candidates that may be sustainably produced for specific and sensitive SARS-CoV-2 serodiagnosis. (**a**) Pre-defined process and protein quality parameters include overall yield after purification, functional binding to the conformation-dependent mAb CR3022 (RBD) or a commercially available anti-NP antibody as verified by biolayer interferometry, as well as glycosylation analysis. Purified monomer (M), dimer (D), and NP full-length protein (FL)-content was determined by HP-SEC. **b-c,** Pre-validation of antigens for serodiagnosis with sera of healthy blood donors collected prior to 2018 (n = 210) and convalescent sera from a COVID cohort (n = 124; see methods for cohort description) with an automatable bead-based, multiplex Luminex serotest. (**b**) Receiver operating characteristic (ROC) curves of the assayed antigens with an indication of the area under the curve (AUC) and 95% confidence interval (CI), (**c**) Seroreactivity of the two cohorts at a final serum dilution of 1:1200. Blank-corrected values are shown. Shades indicate the calculated cut-off yielding a specificity (Sp) of 99.1% for comparison of antigen performance. P-values were calculated by Mann-Whitney U tests.

tRBDs were purified via an immobilized metal affinity chromatography (IMAC) capture followed by a scalable and fast flow-through anion exchange (AIEX) chromatography step, leading to purities of up to 99%. Owing to reproducible highest production yields of functional protein with adequate diagnostic performance and less batch-to-batch variation, we decided to pursue with HEK-expressed tRBD for our further validations.

As the NP of SARS-CoV-1 has been described to be well produced in bacteria [42], we decided to produce the SARS-CoV-2 NP in *Escherichia coli*. We combined two recently developed generic manufacturing strategies, the CASPON (cpCasp2-based platform fusion protein process) technology [8] and the enGenes-X-press technology [7], allowing for high-level soluble expression of heterologous proteins. NP was expressed as a fusion protein with an N-terminally fused CASPON tag that enables affinity purification and can afterwards be efficiently proteolytically removed, thereby generating the authentic N-terminus. High soluble volumetric titres of 3.7 g/L in a growth-decoupled fed-batch production process yielded 730 mg/L NP after purification with a modified CASPON platform process (**Fig. 1a, right panel**). This strategy delivered untagged NP protein at exceptionally high quality (94.6% purity, defined as protein full-length content) after a multi-step-downstream process. The remaining impurities consisted of NP-related fragments and RNA. Residual host cell protein concentration was 0.9 ng/mg NP and dsDNA concentration was 1 μg/mg NP, as determined by De Vos and colleagues [10]. NP has an intrinsic propensity to oligomerize and displays very slow dissociation from the NP-specific antibody (Abcam, ab272852). Therefore, we provide an upper limit for the K_D value, and calculated k_{obs} values as a surrogate kinetic parameter instead (**Fig. 1a, right panel, Fig. S3**). The nucleocapsid protein also presented with excellent AUC values of 0.994 (0.988−0.999) and comparable performance to HEK-derived tRBD. While the seroreactivity profile of pre-COVID sera appeared to

be more heterogenous against the NP than for tRBD, COVID sera demonstrated a more consistent, robust response against the nucleocapsid protein (**Fig 1b, c, right panel**). This comprehensive set of biotechnological and assay performance characteristics prompted us to pursue ELISA test development with HEK-expressed tRBD and bacterially produced NP.

3.2. Assessment of antigen-dependency of false-positive and false-negative results

A set of sera (28−31 convalescence sera from the above tested) that was considered to be particularly challenging since it included 80% of the identified outliers or borderline serum samples, was selected to optimise the conditions for an ELISA with tRBD and NP to maximise sensitivity of the tests. By titration of the coating antigen as well as the seropositive samples we defined our final conditions to be: 6 μg/mL coating antigen and 1:200 serum dilution (data not shown). Using this consensus set of COVID-sera, but different specificity cohorts for both assays, both antigens allowed for highly sensitive antibody detection, yielding 85.7% and 100% sensitivity with the Luminex and ELISA platform, respectively, at the pre-defined consensus specificity criteria (99.1%, Luminex, 92.9% ELISA, **Fig. 2a**). While antigens are covalently coupled to microspheres via their N-terminal and endogenous primary amines, they are passively adsorbed to ELISA plates via hydrophobic as well as electrostatic interaction [43]. With both, physical and chemical immobilization, antigens get immobilized in a randomly oriented manner. Despite previous studies demonstrating good correlation between the results obtained with both methods [44,45], we aimed to verify that the different immobilization mechanisms do not result in major antigenic changes of the tRBD and NP antigens and that we can adopt our learnings from the bead-based antigen pre-validation for the setup of an ELISA.

Fig. 2. Convalescent sera from blood donors with mild to moderate courses of disease indicate an advantage of dual-antigen testing and a correlation of tRBD-specific antibodies with SARS-CoV-2 neutralization. a-d, A small set of convalescent sera (*n* = 28−31, part of the Medical University of Vienna COVID-19-cohort) with described courses of disease was used for in-depth analysis of the ELISA candidate antigens. Pre-COVID-19 sera included blood donor sera (*n* = 210 and *n* = 14) collected in pre-COVID-19 times (see methods for detailed cohort description). (**a**) Seroreactivity of HEK-tRBD and *E. coli*-derived NP as assessed by the Luminex platform and ELISA at serum dilutions of 1:1200 and 1:200, respectively, and the cross-platform correlation of the respective readouts. Data give the mean of blank-corrected values from three independent antigen production batches. Sensitivities with the respective test antigens at the indicated pre-defined specificities were calculated by AUC-analysis of ROC curves, P-values were calculated by Mann-Whitney U tests. **b-c,** Assessment of overlaps in (**b**) false-negative and (**c**) false-positive serum samples identified with both the tRBD or NP antigen in the Luminex and ELISA assay. The cut-offs were set to yield low sensitivity (87.1%, ELISA; 85.,7%, Luminex) or specificity (92.9%, both assays), respectively. Shades are coloured according to the respective antigens (NP: blue, tRBD: pink) and indicate the cut-offs. Numbers in blue and red give the total numbers of false-positives/false-negatives for NP or tRBD, respectively, while purple numbers give samples that are classified as false-positives/-negatives with both antigens. (**d**) Correlation and partial correlation analysis of ELISA anti-tRBD as well as anti-NP levels with neutralization titres obtained with authentic SARS-CoV-2 virus. Partial correlations take the effect of antibody levels towards the respective other antigen into account. Individual sera are color-coded according to the course of disease (green: asymptomatic and mild; black: moderate; red: severe). Solid lines indicate the linear regression and shades with dotted borders give the 95% CI. Full circles are for sera from individuals with a PCR-confirmed SARS-CoV-2 infection, open squares indicate asymptomatic close contacts. r_s, Spearman's correlation factor.

Three independently produced tRBD and NP production batches were tested for seroreactivity with the described panel of COVID-sera using ELISA and Luminex assays. The fluorescence (MFI, Luminex) and colorimetric (OD, ELISA) mean readouts obtained with antigens from three independent production batches demonstrated excellent cross-platform correlation (tRBD: r_s=0.97, p<0.0001; NP: r_s=0.87, p<0.0001, both Spearman correlation) and confirmed that results are in good agreement (**Fig. 2a**). While this does not inform us about potential differences at the resolution of a single-epitope level, it still verifies the equivalence of the assay readouts when using polyclonal serum samples, which is most relevant in our case. Next, we aimed to assess whether false-positive or false-negative results are independent of the test antigen. Thereby, we set the assay cut-offs to either yield low sensitivity or low specificity and then compared whether samples above/below the threshold are shared between the diagnostic antigens. With both test formats, up to 50% of the false-negative samples did not simultaneously react with both antigens (**Fig. 2b**). Concurrently, none of the false-positive sera in the ELISA, and only 20% of the false-positive sera (5 out of 25) in the Luminex test simultaneously reacted with both the tRBD and NP (**Fig. 2c**). Levels of tRBD- and NP-specific antibodies correlated well with each other (r_s=0.75−0.80, p<0.0001, Spearman, **Fig. 2b**) and also with the ability of the respective sera to neutralize authentic SARS-CoV-2 virus. Yet, with partial correlation analysis we could demonstrate that only

anti-tRBD antibodies do have a causal relation with viral neutralization (r_s=0.68, p = 0.0003, Spearman, **Fig. 2d**).

3.3. Cut-off modelling and diagnostic performance of the tests in a large validation cohort

The above data provided an indication that reactivity of COVID-19 sera is dependent on the test antigen, fostering the idea for combined use in applications requiring high specificity. Test kits for both antigens were generated (termed Technozym NP or RBD IgG Test, Technoclone, Vienna, AT), providing the antigens in lyophilized form at a coating concentration of 6 μg/mL. The kits included a five-point calibrator set, based on the RBD-specific antibody CR3022, to enable quantitative readouts and further expand the tests' fields of application.

Both the tRBD and the NP ELISA were evaluated using 244 samples from patients with active or previous SARS-CoV-2 infection covering the full spectrum of disease presentations (asymptomatic to individuals requiring intensive care). The large specificity cohort (*n* = 1126) covered a great variety in samples from pre-COVID times including sera from individuals with rheumatic disease, human coronavirus infections and serum samples drawn during winter months to increase the likelihood for respiratory infections. A detailed description of the SARS-CoV-2 positive cohorts can be found in

Table S1. In ROC-analysis, both assays presented with excellent areas under the curve (tRBD: 0.976, NP: 0.974, Fig. 3a, b). The Youden index was maximal at a cut-off of >2.549 U/mL for tRBD (Youden index=0.901) and at >3.010 U/mL for NP (Youden index=0.882) yielding high sensitivities (tRBD: 95.8% [91.6−97.4], NP: 93.0% [89.1−95.9] at these cut-offs. Yet, specificities (tRBD 95.3% [93.6−96.2], NP 95.1% [93.7−96.3]) were insufficient to yield satisfactory positive predictive values (PPVs), which give the probabilities that an individual with a positive test result indeed has antibodies for SARS-CoV-2. At a low seroprevalence rate of 5% the PPVs at these cut-offs would be equivalent to a coin toss, with 50.2% (43.8−56.5) for tRBD and 50.1% (43.6−56.5) for NP. To increase assay specificity of each test individually, thereby increasing predictability at low seroprevalences, cut-off criteria based on the 99th percentile method were established. Ninety-nine percent of all negative samples showed results below 7.351 (95% CI: 5.733−10.900) U/mL for the tRBD and 7.748 (5.304−11.157) U/mL for the NP ELISA. When shifting the cut-off to 8.000 U/mL (taking a safety margin into account), specificities increased to 99.2% for the tRBD and 99.1% for the NP ELISA. This is a remarkable result for an ELISA test and qualifies the tests for seroprevalence studies. At the same time, sensitivities slightly dropped to

86.3% and 76.7% for the tRBD and NP assays, respectively. The PPVs increased to 84.8% for tRBD and 82.5% for NP (Fig. 3a, b). To monitor of immune responses after infection or vaccination, a cut-off yielding higher sensitivities at acceptable specificities was established. A cut-off between the criteria suggested by the ROC analysis and that calculated by the 99th percentile method, e.g., 5.000 U/mL, yielded a sensitivity of 89.8% and a specificity of 98.0% for the tRBD assay, as well as a sensitivity of 86.5% and a specificity of 98.3% for the NP assay (Fig. 3a, b).

3.4. Orthogonal testing approach at very low seroprevalences to approximate 100% specificity

For low seroprevalences, when specificities need to approximate 100% in order to achieve acceptable PPVs, we considered an orthogonal testing approach (OTA). Our previous experiments already provided an indication that false-positives among pre-COVID-19 sera do not necessarily react with both antigens (Fig. 2c). As a classical OTA might negatively affect sensitivities an adaptive, sensitivity-improved (SI-OTA) was applied [46]. To this end, the above-described validation cohorts were screened with the tRBD ELISA. All samples with results ranging

Cut-off	5.000 U/ml	8.000 U/ml
Sensitivity	86.5 (81.5 - 90.5)	79.5 (73.9 - 84.4)
Specificity	98.3 (97.4 - 99.0)	99.1 (98.4 - 99.6)
PPV (5%)	73.0 (63.3 - 80.9)	82.5 (71.7 - 89.8)
NPV (5%)	99.3 (99.0 - 99.5)	98.9 (98.6 - 99.2)

Cut-off	5.000 U/ml	8.000 U/ml
Sensitivity	89.8 (85.2 - 93.3)	84.4 (79.3 - 88.7)
Specificity	98.0 (97.9 - 98.7)	99.2 (98.5 - 99.6)
PPV (5%)	69.8 (60.6 - 77.6)	99.5 (99.2 - 99.6)
NPV (5%)	84.8 (74.3 - 91.4)	99.2 (98.9 - 99.4)
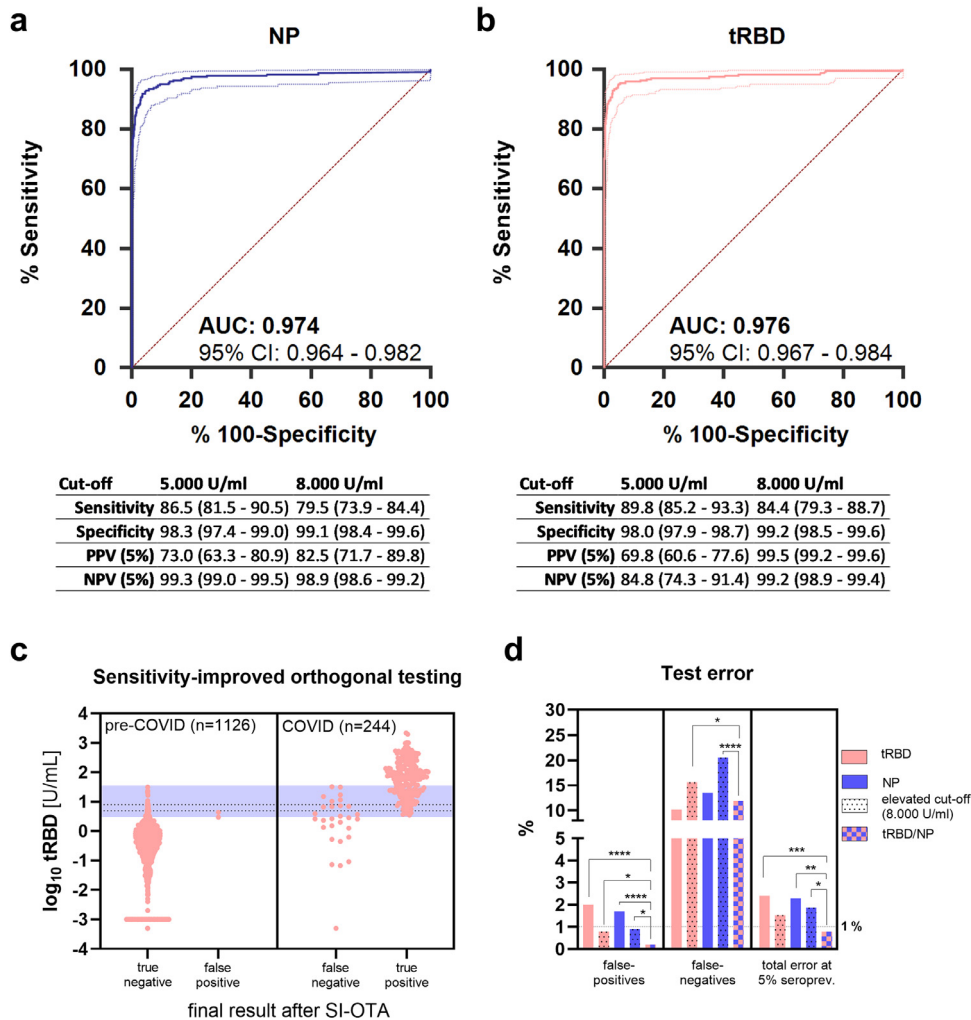
Fig. 3. Performance validation of the Technozym NP and RBD tests. ROC-curve (AUC±95% confidence intervals) of (a) the Technozym RBD- and (b) the NP-ELISA on basis of a cohort of 1126 pre-COVID-19 and 244 COVID-19 serum samples. (c) Results from an adaptive orthogonal testing approach, where all samples yielding <3.000 U/mL in the tRBD ELISA were considered negative and samples with tRBD >35.000 U/mL positive. Samples with tRBD values between those borders were re-tested with the NP ELISA (blue shade). If NP>3.500 U/mL, positivity was confirmed, otherwise it was ruled out. Dashed lines indicate the cut-offs determined by the 99th percentile method (8.000 U/mL) and a reduced cut-off with increased sensitivity (5.000 U/mL, between 99th percentile- and Youden-index criteria) to display the increase in sensitivity gained by the orthogonal test system. (d) Differences in false-positive and -negative test results for different individual and combined test setups were compared by z-tests, total errors at an estimated 5% seroprevalence were compared by χ^2-tests for proportions. PPV, positive predictive value, NPV, negative predictive value. * $P<0.05$, ** $P<0.01$, *** $P<0.001$, **** $P<0.0001$.

between the cut-off defined by the Youden index (including a safety margin, i.e., 3.000 U/mL) and 35.000 U/mL (as no false-positives occurred above 31.500 U/mL) were re-tested with the NP ELISA. There, also the Youden index criterion, adding a safety margin, was applied for positivity (>3.500 U/mL). Samples with <3.000 U/mL in the screening test were considered negative; samples with results between 3.000 U/mL and 35.000 U/mL in the screening tests and at the same time >3.500 U/mL in the confirmation test were considered positive; samples >35.000 U/mL in the screening test were considered positive. Applying these criterions 133 of 1370 samples needed to be re-tested. In turn, this approach led to a significantly enhanced specificity (99.8% [99.4−100.0]) when compared to the tRBD test alone both at a cut-off of 5.000 U/mL (+0.019, P<0.0001, z-test) and 8.000 U/mL (+0.006, P = 0.035, z-test). Compared to the latter, sensitivity (88.1% [83.4−91.9]) was improved (+0.037, p<0.050, z-test) and the PPV rose to 96.3% (86.7−99.1), see **Fig. 3c**. To achieve this improvement, only 133 (i.e., those with tRBD levels between 3.000 and 35.000 U/mL) of the overall 1370 samples needed to be re-tested by the NP assay, resulting in less than 10% increase in testing volume.

3.5. Cross-reactivity of SARS-CoV-2 IgG antibodies with endemic and seasonal coronaviruses

To better characterise our specificity cohorts, we explored the prevalence of antibodies towards common cold coronaviruses and possible cross-reactivities with our assays. To do so, outliers among the pre-COVID-19 cohort were defined as sera with readouts higher than the 75th percentile + 1.5x interquartile range (IQR) of the total cohort seroreactivity towards the SARS-CoV-2 NP or tRBD (outlier NP: n = 17; tRBD: n = 4). Above these cutoffs, all sera from our specificity cohorts reacted strongly with the spike proteins of circulating human coronaviruses (hCoVs) HKU-1, OC43, 229E, and NL63, confirming widespread seroprevalence in the general population (**Fig. 4a, b**). To further characterise the identified outliers among the pre-COVID-19 sera, we calculated their relative IgG signals, set them in relation to a roughly equal number of sera located at the other extreme on the seroreactivity scale (sera with readouts <25th percentile toward the respective antigen) and compared the differences in relative IgG levels to that towards hCoV antigens. Among our pre-validation cohort, sera with highest relative reactivity towards NP (mean difference: 0.88, p<0.0001, One-Way ANOVA with Sidak post hoc test) also demonstrated significantly elevated relative median IgG levels towards the spike protein of HKU-1 (mean difference: 0.13, p = 0.0113, One-Way ANOVA and Sidak post hoc test, **Fig. 4b**). The specificity cohort we used for clinical validation included eight sera from individuals with PCR-confirmed hCoV infection. None of these yielded false-positive readouts at a cutoff of 5.000 U/mL (**Fig. 4c**) at comparably low specificities of 95.3% (tRBD) and 96.1% (NP) (see **Fig. 3a, b**).

3.6. Clinical evaluation of test performance after symptom onset

Diagnostic accuracy of the Technozym NP or RBD IgG Tests was evaluated at different time points after symptom onset in plasma from hospitalised individuals (general ward and intensive care unit
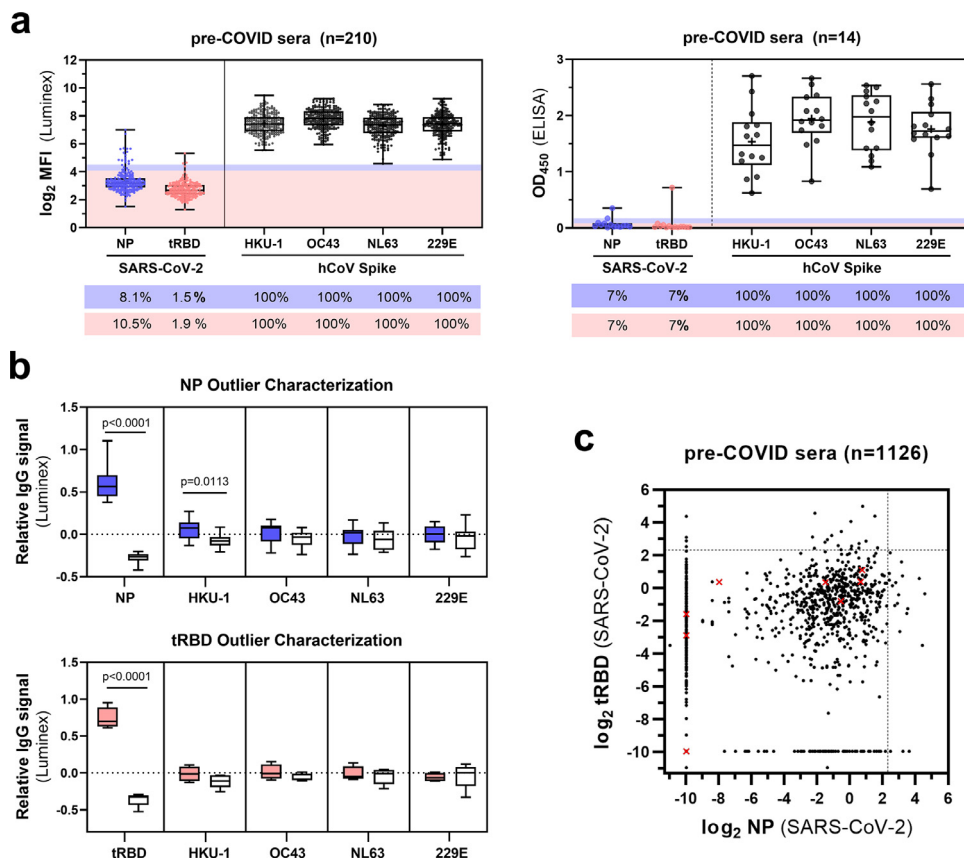
Fig. 4. Characterisation of cross-reactive IgG responses between SARS-CoV-2 and endemic hCoV strains in the specificity cohorts. (a) Seroreactivity of serum samples from the two specificity cohorts (AIT pre-COVID-19 cohort, n = 210 and MedUni Wien Biobank pre-COVID-19, n = 14) employed for pre-validation of the SARS-CoV-2 tRBD and NP antigens with the Luminex or ELISA assays respectively, was measured with the spike proteins of common-cold hCoVs HKU-1, OC43, 229E and NL63. Outliers were classified as observations that fall above the 75th percentile + 1.5 x IQR. Shades give the respective calculated cut-offs and are color-coded for NP (blue) or tRBD (pink). Values below the box-plots give the measured seropositivity in percent. **(b)** Relative IgG levels of NP (n = 17, blue boxes) and tRBD (n = 4, pink boxes) outliers towards the spike proteins of hCoV. White boxes give relative IgG levels of sera with readouts <25th percentile (n = 16 for NP, n = 5 for tRBD) to compare with outliers. Means within groups were compared by One-Way ANOVA followed by a Sidak test to correct for multiple comparisons. **c)** tRBD and NP-specific seroreactivity of the specificity cohort (n = 1126 MedUni Wien Biobank) used for clinical validation. Red crosses display sera from individuals with PCR-confirmed hCoV infection. Dashed lines indicate the cut-off of 5 U/mL.

[ICU] patients) and outpatients. A total of 104 plasma samples were drawn during the acute and early convalescent phase of SARS-CoV-2 infection. NP-specific IgG levels correlated well with tRBD-specific IgG levels, even at levels being below the set threshold for seropositivity (1−5 d: r_s=0.67, p<0.0001; 6−10 d: 0.76, <0.0001; 11−15 d: 0.76, 0.0006, Spearman correlation, **Fig. 5**). The positivity rates increased over time, peaking at 100% 15−22 days after symptom onset in both assays. True positivity rates for the NP ELISA were consistently higher than with the tRBD ELISA at all time points (1−5 d: NP vs tRBD: 14.7% vs 5.9%; 6−10 d: 45.7% vs 34.2%; 11−15 d: 76.5% vs 64.7%, **Fig. 5 and Table S2**). Yet, sera displayed a great heterogeneity in antibody levels throughout the observation period (**Table S2**). None of the false-negative results among the samples were obtained with both assays. Astonishingly, 85.7% of the sera already contained neutralizing antibodies (median titre: 1:24; range 1:4 − 1:128, **Table S2**) as soon as by day five after symptom onset. Of these, however, only a total of 18% of the sera demonstrated seroreactivity above the cut-off for either the NP or tRBD antigen (**Fig. 5**). Yet, the quantitative nature of the assay allowed us to correlate antibody levels below the cut-off for seropositivity and we could demonstrate excellent correlation of tRBD-specific antibodies with neutralizing function at all four investigated time points (1−5 d: r_s=0.49,

p = 0.0004; 6−10 d: r_s=0.77, p <0.0001; 11−15 d: r_s=0.82, p<0.0001; 16−22: r_s=0.67, p = 0.0003, Spearman, **Fig. 5**).

4. Discussion

Superb assay specificity is of utmost importance for the assessment of antibodies directed against SARS-CoV-2, as a substantial proportion of infected individuals escapes identification due to the frequent asymptomatic course of the disease, thereby distorting the true seroprevalence in any given population [47]. The biological basis for false-positives is multifactorial, but the influence of the production platform- and process-related peculiarities or impurities on performance of a diagnostic protein are factors that are often underestimated. While the viral NP is almost exclusively being produced in bacteria [48,49], we expressed the spike receptor binding domain in HEK cells, CHO cells, insect cells and plants [4,50−52]. To find out which of these systems leads to the highest quality and manufacturability of the RBD diagnostic antigen of potentially high demand, we evaluated these production platforms and pre-validated the proteins based on diagnostic performance with a large set of pre-COVID-19 and COVID-19 sera using the Luminex platform. All five expression platforms demonstrated suitability for the production of
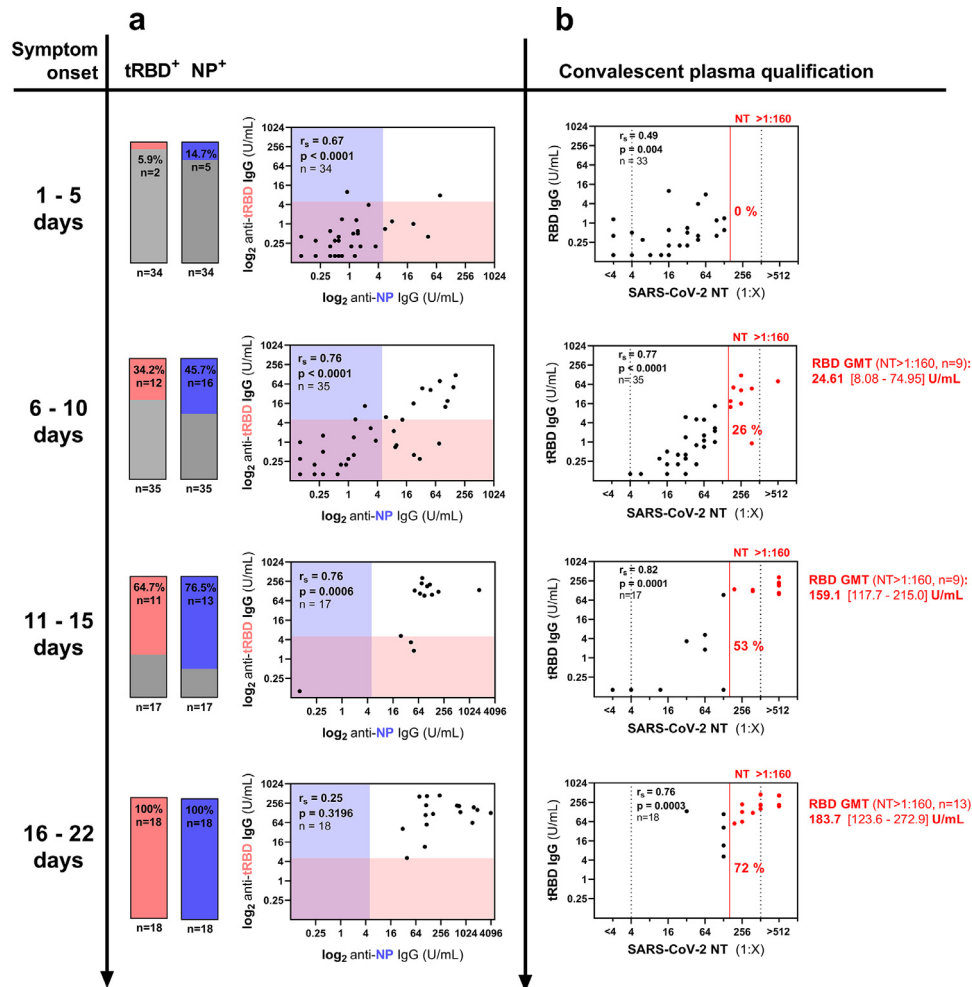
Fig. 5. Time-resolved evaluation of NP, tRBD-specific and neutralizing antibodies in the acute and early convalescent phase after SARS-CoV-2 infection. a-b, A total of 104 plasma samples from 64 outpatients (16%) and hospitalised individuals (65% general ward, ICU 19%) were analyzed for anti-NP and anti-tRBD antibodies and neutralizing antibodies at the indicated time points. (**a**) Antibody levels were assessed with the Technozym ELISAs according to the suggested cut-off of 5.000 U/mL. Bars indicate the fraction of NP, tRBD-positive samples among the tested. Shades give the respective ELISA cut-offs (NP: blue, tRBD: pink). (**b**) Neutralization assays with authentic SARS-CoV-2 virus were performed within a serum dilution range of 1:4 − 1:512 (dashed lines). Values below or above these limits were assigned a titer of 1:2 or 1:1024 for correlation analysis, respectively. The red line indicates a NT of 1:160 that is recommended by the FDA for the screening of recovered COVID-19 patients for convalescent plasma therapy. All sera above this cut-off are color-coded in red. Geometric mean titers and 95% CI in the RBD ELISA are given for sera with a NT >1:160. r_s, Spearman's correlation factor.

functional protein, proven by a binding assay with the SARS-CoV-2-RBD-specific mAb CR3022. Yet, in part due to the different transfection/infection methods used, RBD yields from CHO-K1, CHO-S as well as from *Tnms*42 insect cells and tobacco plants were insufficient for sustainable commercial antigen supply (< 1 mg/L, **Fig. 1**). In contrast, HEK cells readily produced overall yields of 40 mg/L using PEI-transfection. Yields of 30 mg/mL per liter have also been described for CHO-expressed RBD. However, this can be traced back to optimised design of expression constructs and improved production processes for stable RBD-expressing CHO cells together with less extensive purification protocols [53]. We observed higher basal seroreactivity of control sera with insect-derived RBD than with RBD from human and non-human mammalian cell lines; which is in line with other reports [4]. Host-related impurities do not account for that, as insect-cell produced RBD demonstrated the highest purity among all our RBD samples (99%, **Fig. S2**). While there was a common set of false-positive samples shared by RBD from non-human and human mammalian cell lines as well as plants, false-positives reactive with the insect material were entirely insect-RBD-specific (**Fig. S6**). A possible reason may be platform-specific protein modifications, such as glycosylation, that provide the protein with a unique process-derived signature. Indeed, *T. ni*-derived insect cells were demonstrated to generate core α1,3-fucose structures with allergenic potential in humans [54], which might be associated with this peculiar seroreactivity profile.

Based on our observation that RBD tends to form homodimers in an unpredictable manner among different production batches of the same expression host, we used an optimised, truncated version of an RBD as diagnostic antigen (tRBD), enabling the production of large amounts of RBD with consistent quality (**Fig. S2**). For tRBD performance, antigen purity was of utmost importance, even when expressed in human cell lines. A reduction in tRBD purity by 11% (pure: 98.5%, impure: 87.5% purity, **Fig S4a**) resulted in a significant increase in seroreactivity with pre-COVID sera (+0.3, $p<0.0001$, Mann-Whitney test) in the bead-based Luminex assays, while the median fluorescence readouts with COVID sera significantly decreased (-2.5, $p<0.0001$, Mann-Whitney tests). This resulted in a drastic change of the antigens' capability to discriminate the two cohorts and sensitivity decreased by 83.9% (pure: 95.2% versus impure: 11.3% sensitivity, respectively) at a pre-defined consensus specificity of 99.1% (**Fig. S4c**). Since purity after an IMAC capture step was highly batch-dependent and resulted in inconsistent seroreactivity profiles, our standard downstream process included a scalable AIEX chromatography polishing step to account for these inconsistencies and to improve the diagnostic performance of the antigens.

The two test antigens, tRBD from HEK cells and NP from *E. coli*, were further used for ELISA assay development. We configured the assays with a number of sera taken from SARS-CoV-2-infected individuals with weak antibody responses to ensure high assay sensitivity. In contrast to available literature [4,55,56], we used high antigen coating concentrations (6 μg/mL) to yield satisfactory readouts and to achieve a higher dynamic measurement range. A caveat of many assay validation studies is that performance characteristics are skewed by the exclusive inclusion of samples from hospitalised individuals, where robust antibody levels are to be expected [57]. Likewise, the sole consideration of healthy donors in control groups may lead to overestimated assay specificity, as the impact of potential cross-reactive factors present in the general population is largely ignored. In this respect, auto-antibodies commonly found in individuals with inflammatory diseases [58] were already described to cross-react with SARS-CoV-1 antigens [59]. To challenge our tests systems, we biased our large specificity cohort (n = 1126) by including samples with an increased propensity for cross-reactivity, including sera from individuals with inflammatory illnesses (n = 359), sera from PCR-confirmed hCoV infections (n = 8) and sera drawn during winter months to increase the likelihood of respiratory infections

(n = 494). Similarly, our sensitivity cohort (n = 244) included convalescent sera from SARS-CoV-2-infected individuals covering the full spectrum of clinical manifestations (from asymptomatic to ICU patients). Among them, 21% of the sera were collected from asymptomatic individuals or from individuals with mild to moderate illness, who may mount less robust and durable antibody responses after an infection [60]. Based on these cohorts, we defined adequate test parameters to enable highly specific detection of SARS-CoV-2-specific antibodies. A cut-off deduced by the 99th percentile method (8.000 U/mL) allowed for high specific serodiagnosis with 99.2% for the Technozym RBD Test and 99.1% for the Technozym NP Test (at sensitivities of 86.3% and 76.7%, respectively). This is a remarkable result for a tetramethylbenzidine-based manual test system, considering the highly diverse nature of our study cohorts. While some automated systems were described to achieve specificities approximating 100% [61,62], assay performance is highly cohort-specific. The use of diverse study cohorts was also associated with performance deteriorations in such test platforms (i.e. Abbot, Specificity: 97.5%) [63]. For the Meduni Wien Biobank cohort we had performance data with CE-marked automated test systems available [46] to directly compare with our ELISAs at the high specificity cut-off criterion (8.000 U/mL). With an AUC of 0.987 [0.979−0.992] and a specificity of 99.1%, the NP ELISA presented with comparable performance to the Abbott SARS-CoV-2 chemiluminescence microparticle assay (AUC: 0.993 [0.987−0.997], **Fig. S5**, Sp 99.2%) [46], that also relies on the NP antigen. The tRBD ELISA even outperformed the DiaSorin LIAISON® SARS-CoV-2 S1/S2 IgG chemiluminescence assay (tRBD ELISA: AUC/Sp/Sen=0.993/99.2%/84.9% vs DiaSorin:0.976/98.2%/82.8%, see **Fig. S5** and Perkmann and colleagues [46]. While we cannot rule out minor cross-reactivity between hCoV-specific antibodies and SARS-CoV-2 antigens, they appeared to have a limited effect on assay performances (**Fig. 4c**).

Yet, for an estimated seroprevalence of 5% in the general European population [33,64], a test with a specificity and sensitivity of 99.2% and 86.3%, respectively, only scores a PPV of 85.0% resulting in 15 false-positive results out of 100, which is still insufficient. In line with previous results from us and others [34,65,66], we demonstrate that false-positive results are largely antigen-dependent (**Figs. 2b, 4c**). Orthogonal testing is suggested by the Centers of Disease Control and Prevention (CDC) to remedy specificity problems in low transmission settings [67]. Previous studies have used RBD as screening antigen and the trimeric spike protein or the spike S2 domain in second-line tests to confirm initial positive results [4,66]. Such conventional orthogonal test strategies, however, increase specificity often at the expense of sensitivity. We therefore established an adaptive orthogonal test algorithm where positive sera were first identified with the tRBD ELISA allowing for highly sensitive testing (at the expense of specificity) and samples within a predefined area of uncertainty then underwent confirmatory testing with the NP ELISA [46]. This two-test algorithm resulted in a cumulative specificity of 99.8% and an even higher change in sensitivity of 88.1% (+0.037, $p<0.050$, z-test), yielded a PPV of 96.3% [86.7−99.1] (**Fig. 3**). This is an excellent result for a manual test format and its specificity is on par with other orthogonal tests relying on automated systems [46].

As the Technozym NP and RBD ELISAs provide a five-point calibrator set ELISA antibody levels can be quantified, compared and followed over time. For such an application, we chose a cut-off of 5.000 U/mL that allowed for more sensitive analysis of antibody levels at acceptable specificity, adapted from the cut-off given by the Youden index. With convalescent sera taken at median 43−54 days post-symptom onset, the tRBD ELISA allowed for a more sensitive detection of antibodies than the NP ELISA (**Fig. 3a, b**). Yet, time-resolved analysis of seroconversion demonstrated that NP-specific antibodies develop earlier after an infection and true positive rates were consistently higher with the NP ELISA for samples collected within the first 15 days post-symptom onset (**Fig. 5, Table S2**). This

phenomenon has already been described in patients infected with SARS-CoV-1 [68,69] and was associated with higher sensitivities of other SARS-CoV-2 test systems, relying on the NP, in the early phase after an infection [70]. Determining the neutralizing capacity of SARS-CoV-2 anti-RBD antibodies is critical to elucidate possible protective effects of the immune response. Considering all neutralizing activity above background as positive, we observed neutralizing antibodies in 85% of the sera already by day five after symptom onset (**Fig. 5**), which is in line with previous studies [71,72]. Of note, RBD-seroconversion, defined by IgG antibody levels above a threshold of 5.000 U/mL, was observed for only 6% of the sera at this time point. Yet, despite 33 out of 35 samples demonstrating reactivity below our pre-defined cutoff, neutralizing titers correlated well with RBD-specific IgG responses. A recent study demonstrated that the early neutralizing response is dominated by RBD-specific IgA antibodies [73]. As we exclusively measured RBD-specific IgG responses we cannot rule out that part of the early neutralizing activity we observe derive from neutralizing IgA or even earlier IgM responses.

Tests for the screening of reconvalescent COVID-19 patients for the presence of anti-SARS-CoV-2 antibodies are of great interest for identifying suitable donors for convalescent plasma therapy [74]. A retrospective, propensity score−matched case−control study performed at the Mount Sinai hospital (New York, NY) provides evidence for a survival benefit in patients receiving convalescent plasma transfusion as an effective intervention in COVID-19 [74]. In August 2020, the FDA issued a new guidance on the Emergency Use Authorization (EUA) for COVID-19 convalescent plasma, recommending plasma donations to be qualified by either the Mount Sinai COVID-19 ELISA IgG Antibody Test or Ortho VITROS IgG assay [75]. Prior to this guidance, NTs of at least 1:160 were considered acceptable in the absence of high-titer samples [76]. As we did not have the beforementioned tests available, we qualified plasma donors according to the NT 1:160 criterion. The fraction of samples exceeding this threshold gradually increased over time and by day 15 after symptom onset, 53% of the sera and by day 22, 72% of sera had titers higher than 1:160 (**Fig. 5, Table S2**). The geometric mean RBD titers in these sera corresponded to 159.1 U/mL and 183.7 U/mL, respectively. Since correlates of protection from infection remain to be determined we cannot deduce whether these titers are clinically relevant in prophylaxis, at this point.

In conclusion, we have developed two highly specific, quantitative, easy-to-implement and now commercially available SARS-CoV-2 antibody tests and defined optimal thresholds for their application in different aspects of clinical use. We established tailor-made testing algorithms to maximize test performance in a wide range of applications of clinical utility, such as the follow-up of patients after an infection (which demand high sensitivity), but also developed a sensitivity-improved orthogonal testing algorithm for seroprevalence studies (which demand high specificity). Comprehensive test validation with large multi-center cohorts and neutralization assays indicated that our simple, but well-designed tests even outperforms commercially available automated CE-marked test systems with challenging human serum samples. Yet, a dual-testing approach also enables to differentiate between vaccinated and infected individuals, valid for all vaccines not triggering NP responses, or to study the rate of re-infection in people that had been infected or vaccinated. Moreover, the RBD ELISA allows for the identification of donors for convalescent plasma therapy as RBD-specific antibody levels correlate well with the induction of functional neutralization responses. Both tests allow to comprehensively monitor the dynamics of antibody responses after infection. Yet, our data disclose different kinetics for antigen-specific antibody responses, which affect their performance at different time points after an infection. These findings are essential for ongoing efforts to establish serological tests for clinical diagnostics. In this respect, also test performance with convalescent sera collected more than two months after infection and the effect of antigen-specific antibody waning should be carefully addressed in future studies and compared to the comprehensive findings of this study.

Contributors

A.J.,A.W.,C.J.B.,E.L.,F.E.,F.G.,G.S.,G.W.K.,H.H.,J.M.,M.S.,M.D.,M.W.,M.K.,M.C.P.,N.L.,N.Bo.,N.Bi.,P.P.A., R.G.,T.P.,W.G. designed study concepts. A.J.,A.W.,C.J.B,F.E.,F.G.,G.S.,J.M.,M.W.,M.K.,M.C.P.,N.Bi.,R.G.,W.G. acquired financial support for this project. A.W.,B.H.,B.D.,C.J.B,E.G.,E.L.,F.G.,G.M.,G.S.,G.SM.,G.W.K.,H.H.,J.H.,J.B.,J.M.,Li.M.,M.H.,M.E.,M.S.,M.D.,M.W.,M.K.,M.C.P.,N.L.,N.M.,N.Bi.,P.P.A.,P.S.,R.H.,R.G.,Ri.S.,T.P.,W.G. developed and designed methodology . A.E.E.,A.G.,A.W.,B.H.,B.D.,C.I.,C.J.B,C.K.,C.T.,C.G,G.D.M.,D.S.,E.G.,E.L.,F.S.,G.M.,G.L.,G.SM.,G.W.K.,G.H., J.H.,J.D.V.,J.L.R.,J.B.,Lu.M.,M.H.,M.S.,M.K.B.,M.D.,M.W.,M.K.,N.L.,N.M.,N.Bi.,P.P.A.,P.Q.,P.S.,R.H.,R.G.,Ri.S.,Ro.S.,R.B.W.,T.P.,U.V. conducting a research and investigation process, specifically performing the experiments, or data/evidence collection. K.V. developed evaluation software code. A.E.E.,A.G.,B.D.,C.I.,F.G.,G.H.,H.H.,M.D.,M.K.,R.B.W.,T.P. performed data curation. A.W.,F.G.,H.H.,J.H.,M.H.,M.S.,M.K.,W.G. performed data validation and evaluated data reproducibility. B.D.,H.H.,M.D.,M.K. verified the underlying data. A.E.E.,A.G.,A.W.,B.H.,B.D.,C.I.,C.G.G,D.M,E.L.,F.G.,G.M.,G.SM.,G.W.K.,G.H.,H.H.,J.D.V.,K.V.,Lu.M.,M.E., M.D.,M.K.,M.C.P.,N.L.,P.P.A.,Ri.S. applied statistical, mathematical, computational, or other formal techniques to analyze or synthesize study data. H.H.,M.D.,M.K.,R.B.W. performed data visualization. A.E.E.,A.J.,A.G.,C.I.,C.J.B,D.S.,E.L.,F.E.,F.G.,G.S.,G.L.,G.H.,G.W.,J.D.V.,J.L.R.,J.M.,Lu.M.,M.K.B.,M.W.,M.C.P.,N.Bo.,N.Bi.,P.Q.,R.H.,R.G.,Ro.S.,R.B.W.,W.G., provided study materials, reagents, laboratory samples, animals, instrumentation, computing resources, or other analysis tools. A.W.,C.J.B,F.G.,G.S.,G.W.,Lu.M.,M.C.P,M.D.,M.K.,N.Bo.,N.Bi.,R.G.,R.B.W.,W.G. were responsible for supervising research activities and for project administration. H.H.,M.D.,M.K.,M.C.P.,R.G.,T.P. wrote the original draft. B.D.,C.J.B,E.L.,F.G.,G.W.K.,J.D.V.,J.M.,Lu.M.,M.E.,M.C.P.,N.L.,P.P.A.,P.S.,R.G.,W.G. reviewed and edited the manuscript. All authors read and approved the final version of the manuscript and have had access to the raw data.

Data sharing statement

All data needed to evaluate the conclusions in the paper are present in the manuscript and/or the Supplementary Materials. Further information on the study protocol will be made available to interested researchers. Recombinant SARS-CoV-2 antigens can be requested from interested researchers for research purposes under www.boku-covid19.at (after registration). For commercial purposes antigens can be requested from enGenes Biotech GmbH. Technozym NP and RBD IgG serotests are available from Technoclone (Technoclone Herstellung von Diagnostika und Arzneimitteln GmbH, Vienna, Austria).

Declaration of Competing Interest

Dr. Klausberger has nothing to disclose. Dr. Duerkop has nothing to disclose. Dr. Haslacher has nothing to disclose. Dr. Wozniak-Knopp has nothing to disclose. Dr. Cserjan-Puschmann has nothing to disclose. Dr. Perkmann has nothing to disclose. Dr. Lingg has nothing to disclose. Dr. Pereira Aguilar has nothing to disclose. Dr. Laurent has nothing to disclose. Dr. De Vos has nothing to disclose. Mag.rer.nat. Hofner has nothing to disclose. Dr. Holzer has nothing to disclose. Mrs. Stadler has nothing to disclose. Dipl.-Ing. Manhart has nothing to disclose. DI Vierlinger has nothing to disclose. Dr. Egger has nothing to disclose. Dipl. Ing. Milchram has nothing to disclose. Dr. Gludovacz has nothing to disclose. Dr. Marx has nothing to disclose. Dipl.-Ing. Köppl has nothing to disclose. Christopher Tauer, BSc has nothing to disclose. Jürgen Beck, MSc reports nothing to disclose. Daniel

Acknowledgments

Supplementary materials

Supplementary material associated with this article can be found in the online version at doi:10.1016/j.ebiom.2021.103348.

References

[1] Long Q-X, Liu B-Z, Deng H-J, Wu G-C, Deng K, Chen Y-K, et al. Antibody responses to SARS-CoV-2 in patients with COVID-19. Nat Med 2020;26(6):845–8 Jun.

[2] Foundation for Innovative New Diagnostics (FIND). SARS-CoV-2 diagnostic pipeline. [cited 2021 Mar 11]; Available from: https://www.finddx.org/covid-19/pipeline/?avance=Commercialized&type=Manual+or+automated+immunoassays&test_target=Antibody&status=all&section=immunoassays&action=default#diag_tab

[3] Lisboa Bastos M, Tavaziva G, Abidi SK, Campbell JR, Haraoui L-P, Johnston JC, et al. Diagnostic accuracy of serological tests for covid-19: systematic review and meta-analysis. BMJ 2020;1:m2516. Jul.

[4] Amanat F, Stadlbauer D, Strohmeier S, Nguyen THO, Chromikova V, McMahon M, et al. A serological assay to detect SARS-CoV-2 seroconversion in humans. Nat Med 2020;26(7):1033–6 Jul.

[5] Wu F, Zhao S, Yu B, Chen Y-M, Wang W, Song Z-G, et al. A new coronavirus associated with human respiratory disease in China. Nature 2020;579(7798):265–9 Mar.

[6] Sainsbury F, Thuenemann EC, Lomonossoff GP. pEAQ: versatile expression vectors for easy and quick transient expression of heterologous proteins in plants. Plant Biotechnol J 2009;7(7):682–93 Sep.

[7] Stargardt P, Feuchtenhofer L, Cserjan-Puschmann M, Striedner G, Mairhofer J. Bacteriophage inspired growth-decoupled recombinant protein production in Escherichia coli. ACS Synth Biol 2020;9(6):1336–48 Jun 19.

[8] Cserjan-Puschmann M, Lingg N, Engele P, Kröß C, Loibl J, Fischer A, et al. Production of circularly permuted caspase-2 for affinity fusion-tag removal: cloning, expression in Escherichia coli, purification, and characterization. Biomolecules 2020;10(12):1592. Nov 24.

[9] Lingg N., Cserjan-Puschmann M., Fischer A., Engele P., Kröß C., Schneider R., et al. Advanced purification platform using circularly permuted caspase-2 for affinity fusion-tag removal to produce native fibroblast growth factor 2. J Chem Technol Biotechnol [Internet]. 2021 Jan 27 [cited 2021 Mar 11]; Available from: https://onlinelibrary.wiley.com/ 10.1002/jctb.6666

[10] DeVos J., Pereira Aguilar P., Köppl C., Fischer A., Grünwald-Gruber C., Dürkop M., et al. Native hydrophobic interaction chromatography hyphenated to multi-angle light scattering detection for in-process control of SARS-CoV-2 nucleocapsid protein produced in Escherichia Coli. 2021 Mar 11 [cited 2021 Mar 11]; Available from: 10.26434/chemrxiv.14195318.v1

[11] Tian X, Li C, Huang A, Xia S, Lu S, Shi Z, et al. Potent binding of 2019 novel coronavirus spike protein by a SARS coronavirus-specific human monoclonal antibody. Emerg Microbes Infect 2020;9(1):382–5 Jan 1.

[12] Mairhofer J, Cserjan-Puschmann M, Striedner G, Nöbauer K, Razzazi-Fazeli E, Grabherr R. Marker-free plasmids for gene therapeutic applications—Lack of antibiotic resistance gene substantially improves the manufacturing process. J Biotechnol 2010;146(3):130–7 Apr 1.

[13] Urthaler J, Ascher C, Wöhrer H, Necina R. Automated alkaline lysis for industrial scale cGMP production of pharmaceutical grade plasmid-DNA. J Biotechnol 2007;128(1):132–49 Jan.

[14] Cytiva. Application Note 28-4094-85 AA: PlasmidSelect Xtra for downstream processing of supercoiled plasmid DNA. 2020 Jul.

[15] Durocher Y. High-level and high-throughput recombinant protein production by transient transfection of suspension-growing human 293-EBNA1 cells. Nucl Acids Res 2002;30(2):9e–9 Jan 15.

[16] Lobner E, Humm A-S, Göritzer K, Mlynek G, Puchinger MG, Hasenhindl C, et al. Fcab-HER2 interaction: a Ménage à Trois. Lessons from X-Ray and solution studies. Structure 2017;25(6):878–89 June5.

[17] Chen Y-R, Zhong S, Fei Z, Hashimoto Y, Xiang JZ, Zhang S, et al. The transcriptome of the Baculovirus Autographa Californica Multiple Nucleopolyhedrovirus in Trichoplusia ni cells. J Virol 2013;87(11):6391–405 Jun 1.

[18] Koczka K, Peters P, Ernst W, Himmelbauer H, Nika L, Grabherr R. Comparative transcriptome analysis of a Trichoplusia ni cell line reveals distinct host responses to intracellular and secreted protein products expressed by recombinant baculoviruses. J Biotechnol 2018;270:61–9 Mar.

[19] Klausberger M, Wilde M, Palmberger D, Hai R, Albrecht RA, Margine I, et al. One-shot vaccination with an insect cell-derived low-dose influenza A H7 virus-like particle preparation protects mice against H7N9 challenge. Vaccine 2014;32 (3):355–62 Jan.

[20] Strasser R, Stadlmann J, Schähs M, Stiegler G, Quendler H, Mach L, et al. Generation of glyco-engineered Nicotiana benthamiana for the production of monoclonal antibodies with a homogeneous human-like N-glycan structure: XylT and FucT down-regulation in N. benthamiana. Plant Biotechnol J 2008;6(4):392–402 May.

[21] Castilho A, Gattinger P, Grass J, Jez J, Pabst M, Altmann F, et al. N-Glycosylation engineering of plants for the biosynthesis of glycoproteins with bisected and branched complex N-glycans. Glycobiology 2011;21(6):813–23 Jun.

[22] Göritzer K, Turupcu A, Maresch D, Novak J, Altmann F, Oostenbrink C, et al. Distinct Fcα receptor N -glycans modulate the binding affinity to immunoglobulin A (IgA) antibodies. J Biol Chem 2019;294(38):13995–4008 Sep 20.

[23] Hulme EC, Trevethick MA. Ligand binding assays at equilibrium: validation and interpretation: equilibrium binding assays. Br J Pharmacol 2010;161(6):1219–37 Nov.

[24] Armbruster DA, Pry T. Limit of blank, limit of detection and limit of quantitation. Clin Biochem Rev 2008;29(Suppl 1):S49–52 Aug.

[25] Carvalho SB, Moreira AS, Gomes J, Carrondo MJT, Thornton DJ, Alves PM, et al. A detection and quantification label-free tool to speed up downstream processing of model mucins editor D'Auria S, editor. A detection and quantification label-free tool to speed up downstream processing of model mucins. PLoS One 2018;13(1): e0190974 Jan 9.

[26] Klein JS, Bjorkman PJ. Few and far between: how HIV may be evading antibody avidity editor Rall GF, editor. Few and far between: how HIV may be evading antibody avidity. PLoS Pathog 2010;6(5):e1000908 May 27.

[27] Hattori T, Lai D, Dementieva IS, Montaño SP, Kurosawa K, Zheng Y, et al. Antigen clasping by two antigen-binding sites of an exceptionally specific antibody for histone methylation. Proc Natl Acad Sci 2016;113(8):2092–7 Feb 23.

[28] Wallner J, Lhota G, Schosserer M, Vorauer-Uhl K. An approach for liposome immobilization using sterically stabilized micelles (SSMs) as a precursor for biolayer interferometry-based interaction studies. Colloids Surf B 2017;154:186–94 Jun.

[29] Katsamba PS, Navratilova I, Calderon-Cacia M, Fan L, Thornton K, Zhu M, et al. Kinetic analysis of a high-affinity antibody/antigen interaction performed by multiple biacore users. Anal Biochem 2006;352(2):208–21 May.

[30] Abdiche YN, Malashock DS, Pons J. Probing the binding mechanism and affinity of tanezumab, a recombinant humanized anti-NGF monoclonal antibody, using a repertoire of biosensors. Protein Sci 2008;17(8):1326–35 Aug.

[31] Irsara C, Egger A.E., Prokop W., Nairz M., Loacker L, Sahanic S., et al. Evaluation of four commercial, fully automated SARS-CoV-2 antibody tests suggests a revision of the Siemens SARS-CoV-2 IgG assay. Clin Chem Lab Med (CCLM) [Internet]. [cited 2021 Mar 11];0(0). Available from: https://www.degruyter.com/view/journals/cclm/ahead-of-print/article-10.1515-cclm-2020-1758/article-10.1515-cclm-2020-1758.xml

[32] Buderer NMF. Statistical methodology: I. Incorporating the prevalence of disease into the sample size calculation for sensitivity and specificity. Acad Emerg Med 1996;3(9):895–900 Sep.

[33] Statistik Austria, Medical University of Vienna. In the middle/end of October 2020, 4.7% of the Austrian population had antibodies to SARS-CoV-2. Extrapolation of Austria-wide COVID 19 prevalence study [Internet]. [cited 2021 Mar 11]. Available from: https://www.meduniwien.ac.at/web/en/ueber-uns/news/detailseite/2020/news-im-dezember-2020/47-der-oesterreichischen-bevoelkerung-hatten-mitte/ende-oktober-2020-antikoerper-gegen-sars-cov-2/

[34] Perkmann T, Perkmann-Nagele N, Breyer M-K, Breyer-Kohansal R, Burghuber OC, Hartl S, et al. Side-by-side comparison of three fully automated SARS-CoV-2 antibody assays with a focus on specificity. Clin Chem 2020;66 (11):1405–13 Nov 1.

[35] Frey A, Di Canzio J, Zurakowski D. A statistically defined endpoint titer determination method for immunoassays. J Immunol Methods 1998;221(1–2):35–41 Dec.

[36] Breyer-Kohansal R, Hartl S, Burghuber OC, Urban M, Schrott A, Agusti A, et al. The LEAD (Lung, Heart, Social, Body) study: objectives, methodology, and external validity of the population-based cohort study. J Epidemiol 2019;29(8):315–24 Aug 5.

[37] Haslacher H, Gerner M, Hofer P, Jurkowitsch A, Hainfellner J, Kain R, et al. Usage data and scientific impact of the prospectively established fluid bioresources at the hospital-based MedUni Wien Biobank. Biopreserv Biobanking 2018;16 (6):477–82 Dec.

[38] Hoffmann M, Kleine-Weber H, Schroeder S, Krüger N, Herrler T, Erichsen S, et al. SARS-CoV-2 cell entry depends on ACE2 and TMPRSS2 and is blocked by a clinically proven protease inhibitor. Cell 2020;181(2):271–80 Apre8.

[39] Laferl H., Kelani H., Seitz T., Holzer B., Zimpernik I., Steinrigl A., et al. An approach to lifting self-isolation for health care workers with prolonged shedding of SARS-CoV-2 RNA. Infection. 2020 Oct 6;

[40] Reed LJ, Muench H. A simple method of estimating fifty per cent endpoints12. Am J Epidemiol 1938;27(3):493–7 May.

[41] Beck JR, Shultz EK. The use of relative operating characteristic (ROC) curves in test performance evaluation. Arch Pathol Lab Med 1986;110(1):13–20 Jan.

[42] Pei H, Liu J, Cheng Y, Sun C, Wang C, Lu Y, et al. Expression of SARS-coronavirus nucleocapsid protein in Escherichia coli and Lactococcus lactis for serodiagnosis and mucosal vaccination. Appl Microbiol Biotechnol 2005;68(2):220–7 Aug.

[43] Welch NG, Scoble JA, Muir BW, Pigram PJ. Orientation and characterization of immobilized antibodies for improved immunoassays (Review). Biointerphases 2017;12(2):02D301. Jun.

[44] Elshal MF, McCoy JP. Multiplex bead array assays: performance evaluation and comparison of sensitivity to ELISA. Methods 2006;38(4):317–23 Apr.

[45] Tyson J, Tsai W-Y, Tsai J-J, Mässgård L, Stramer SL, Lehrer AT, et al. A high-throughput and multiplex microsphere immunoassay based on non-structural protein 1 can discriminate three flavivirus infections editor Gubler DJ, editor. A high-throughput and multiplex microsphere immunoassay based on non-structural protein 1 can discriminate three flavivirus infections. PLoS NeglTrop Dis 2019;13(8):e0007649 Aug 23.

[46] Perkmann T., Perkmann-Nagele N., Oszvar-Kozma M., Koller T., Breyer M.-K., Breyer-Kohansal R., et al. Increasing both specificity and sensitivity of SARS-CoV-2 antibody tests by using an adaptive orthogonal testing approach [Internet]. [cited 2021 Mar 11]. Available from: http://medrxiv.org/lookup/ 10.1101/2020.11.05.20226449

[47] Yong SEF, Anderson DE, Wei WE, Pang J, Chia WN, Tan CW, et al. Connecting clusters of COVID-19: an epidemiological and serological investigation. Lancet Infect Dis 2020;20(7):809–15 Jul.

[48] Yue L, Cao H, Xie T, Long R, Li H, Yang T, et al. N-terminally truncated nucleocapsid protein of SARS-CoV-2 as a better serological marker than whole nucleocapsid protein in evaluating the immunogenicity of inactivated SARS-CoV-2. J Med Virol 2021;93(3):1732–8 Mar.

[49] Rump A, Risti R, Kristal M-L, Reut J, Syritski V, Lookene A, et al. Dual ELISA using SARS-CoV-2 nucleocapsid protein produced in E. coli and CHO cells reveals epitope masking by N-glycosylation. Biochem Biophys Res Commun 2021;534:457–60 Jan 1.

[50] Das D, Suresh MR. Copious production of SARS-CoV nucleocapsid protein employing codon optimized synthetic gene. J Virol Methods 2006;137(2):343–6 Nov.

[51] Pino P, Kint J, Kiseljak D, Agnolon V, Corradin G, Kajava AV, et al. Trimeric SARS-CoV-2 spike proteins produced from CHO cells in bioreactors are high-quality antigens. Processes 2020;8(12):1539. Nov 25.

[52] Rattanapisit K, Shanmugaraj B, Manopwisedjaroen S, Purwono PB, Siriwattananon K, Khorattanakulchai N, et al. Rapid production of SARS-CoV-2 receptor binding domain (RBD) and spike specific monoclonal antibody CR3022 in Nicotiana benthamiana. Sci Rep 2020;10(1) [Internet]Dec [cited 2021 Mar 11]Available from: http://www.nature.com/articles/s41598-020-74904-1.

[53] Sinegubova MV, Orlova NA, Kovnir SV, Dayanova LK, Vorobiev II. High-level expression of the monomeric SARS-CoV-2 S protein RBD 320-537 in stably transfected CHO cells by the EEF1A1-based plasmid vector editor Ho PL, editor. High-level expression of the monomeric SARS-CoV-2 S protein RBD 320-537 in stably transfected CHO cells by the EEF1A1-based plasmid vector. PLoS One 2021;16(2): e0242890 Feb 2.

[54] Palmberger D, Ashjaei K, Strell S, Hoffmann-Sommergruber K, Grabherr R. Minimizing fucosylation in insect cell-derived glycoproteins reduces binding to IgE antibodies from the sera of patients with allergy. Biotechnol J 2014;9(9):1206–14 Sep.

[55] Roy V, Fischinger S, Atyeo C, Slein M, Loos C, Balazs A, et al. SARS-CoV-2-specific ELISA development. J Immunol Methods 2020;484−485:112832 Sep.

[56] Alandijany TA, El-Kafrawy SA, Tolah AM, Sohrab SS, Faizo AA, Hassan AM, et al. Development and optimization of in-house ELISA for detection of human IgG antibody to SARS-CoV-2 full length spike protein. Pathogens 2020;9(10):803. Sep 28.

[57] Marklund E, Leach S, Axelsson H, Nyström K, Norder H, Bemark M, et al. Serum-IgG responses to SARS-CoV-2 after mild and severe COVID-19 infection and analysis of IgG non-responders editor Walsh SR, editor. Serum-IgG responses to SARS-CoV-2 after mild and severe COVID-19 infection and analysis of IgG non-responders. PLoS One 2020;15(10):e0241104 Oct 21.

[58] Kang EH, Ha Y-J, Lee YJ. Autoantibody biomarkers in rheumatic diseases. Int J Mol Sci 2020;21(4):1382. Feb 18.

[59] Wang Y, Sun S, Shen H, Jiang L, Zhang M, Xiao D, et al. Cross-reaction of SARS-CoV antigen with autoantibodies in autoimmune diseases. Cell Mol Immunol 2004;1 (4):304–7 Aug.

[60] Long Q-X, Tang X-J, Shi Q-L, Li Q, Deng H-J, Yuan J, et al. Clinical and immunological assessment of asymptomatic SARS-CoV-2 infections. Nat Med 2020;26 (8):1200–4 Aug.

[61] Bryan A, Pepper G, Wener MH, Fink SL, Morishima C, Chaudhary A, et al. Performance characteristics of the Abbott architect SARS-CoV-2 IgG assay and Seroprevalence in Boise, Idaho editor McAdam AJ, editor. Performance characteristics of the Abbott architect SARS-CoV-2 IgG assay and Seroprevalence in Boise, Idaho. J Clin Microbiol 2021;58(8).

[62] Harley K, Gunsolus IL. Comparison of the clinical performances of the Abbott alinity IgG, Abbott architect IgM, and Roche Elecsys total SARS-CoV-2 antibody assays editor Tang Y-W, editor. Comparison of the clinical performances of the Abbott alinity IgG, Abbott architect IgM, and Roche Elecsys total SARS-CoV-2 antibody assays. J Clin Microbiol 2020;59(1):e02104–20 Dec 17.

[63] Jääskeläinen A, Kuivanen S, Kekäläinen E, Ahava M, Loginov R, Kallio-Kokko H, et al. Performance of six SARS-CoV-2 immunoassays in comparison with microneutralisation. J Clin Virol 2020;129:104512 Aug.

[64] Rostami A, Sepidarkish M, Leeflang MMG, Riahi SM, Nourollahpour Shiadeh M, Esfandyari S, et al. SARS-CoV-2 seroprevalence worldwide: a systematic review and meta-analysis. Clin Microbiol Infect 2021;27(3):331–40 Mar.

[65] Pflüger LS, Bannasch JH, Brehm TT, Pfefferle S, Hoffmann A, Nörz D, et al. Clinical evaluation of five different automated SARS-CoV-2 serology assays in a cohort of hospitalized COVID-19 patients. J Clin Virol 2020;130:104549 Sep.

[66] Ripperger TJ, Uhrlaub JL, Watanabe M, Wong R, Castaneda Y, Pizzato HA, et al. Orthogonal SARS-CoV-2 serological assays enable surveillance of low-prevalence communities and reveal durable humoral immunity. Immunity 2020;53(5):925–33 Nove4.

[67] CDC Centers for Disease Control and Prevention. Interim guidelines for COVID-19 antibody testing in clinical and public health settings [Internet]. 2020 Jan [cited 2021 Mar 11]. Available from: https://www.cdc.gov/coronavirus/2019-ncov/lab/resources/antibody-tests-guidelines.html

[68] Woo PCY, Lau SKP, Wong BHL, Tsoi H -w, Fung AMY, Kao RYT, et al. Differential sensitivities of severe acute respiratory syndrome (SARS) coronavirus spike polypeptide enzyme-linked immunosorbent assay (ELISA) and SARS coronavirus nucleocapsid protein ELISA for serodiagnosis of SARS coronavirus pneumonia. J Clin Microbiol 2005;43(7):3054–8 Jul 1.

[69] Tan Y-J, Goh P-Y, Fielding BC, Shen S, Chou C-F, Fu J-L, et al. Profiles of antibody responses against severe acute respiratory syndrome coronavirus recombinant proteins and their potential use as diagnostic markers. Clin Diagn Lab Immunol 2004;11(2):362–71 Mar.

[70] Turbett SE, Anahtar M, Dighe AS, Garcia Beltran W, Miller T, Scott H, et al. Evaluation of three commercial SARS-CoV-2 serologic assays and their performance in two-test algorithms Editors Caliendo AM, editor. Evaluation of three commercial SARS-CoV-2 serologic assays and their performance in two-test algorithms. J Clin Microbiol 2020;59(1) Oct 5.

[71] Suthar MS, Zimmerman MG, Kauffman RC, Mantus G, Linderman SL, Hudson WH, et al. Rapid generation of neutralizing antibody responses in COVID-19 patients. Cell Rep Med 2020;1(3):100040 Jun.

[72] Wu F, Liu M, Wang A, Lu L, Wang Q, Gu C, et al. Evaluating the association of clinical characteristics with neutralizing antibody levels in patients who have recovered from mild COVID-19 in Shanghai, China. JAMA Intern Med 2020;180(10):1356. Oct 1.

[73] Sterlin D, Mathian A, Miyara M, Mohr A, Anna F, Claër L, et al. IgA dominates the early neutralizing antibody response to SARS-CoV-2. Sci Transl Med 2020;7: eabd2223. Dec.

[74] Liu STH, Lin H-M, Baine I, Wajnberg A, Gumprecht JP, Rahman F, et al. Convalescent plasma treatment of severe COVID-19: a propensity score−matched control study. Nat Med 2020;26(11):1708–13 Nov.

[75] Food and Drug Administration (FDA). Recommendations for investigational COVID-19 convalescent plasma [Internet]. 2020 [cited 2021 Mar 11]. Available from: https://www.fda.gov/vaccines-blood-biologics/investigational-new-drug-ind-or-device-exemption-ide-process-cber/recommendations-investigational-covid-19-convalescent-plasma#compliance

[76] Lee WT, Girardin RC, Dupuis AP, Kulas KE, Payne AF, Wong SJ, et al. Neutralizing antibody responses in COVID-19 convalescent sera. J Infect Dis 2021;223(1):47–55 Jan 4.